REVIEWS in MINERALOGY
Volume 34

REACTIVE TRANSPORT IN POROUS MEDIA

P.C. LICHTNER, C.I. STEEFEL
& E.H. OELKERS, *Editors*

Series Editor: Paul H. Ribbe
MINERALOGICAL SOCIETY OF AMERICA

Chapter 4

MULTICOMPONENT ION EXCHANGE AND CHROMATOGRAPHY IN NATURAL SYSTEMS

C. A. J. Appelo
Faculty of Earth Sciences, Free University
De Boelelaan 1085
1081 HV Amsterdam, The Netherlands

INTRODUCTION

Ritchie (1966) noted that it was a geologic setting that first evoked the need for a chromatographic explanation. He was referring to experiments by soil chemists who in the middle of the 19th century measured the exchange of NH_4^+ versus Ca^{2+} in soil samples. Ritchie then continued to lament that geologists are reluctant to accept the concepts of chromatography, and he invited chromatographers to apply their expertise to geological problems. Multicomponent ion exchange was indeed not given much attention in geochemistry, and soil chemistry textbooks that explain how to calculate multicomponent exchange equilibria are still rare.

There is, on the other hand, not one soil scientist who will deny the importance of ion exchange in regulating soil solution compositions. It is not reluctance to apply chromatographic theory in soil science, but rather the feeling that processes are more complicated than can be solved by the relatively simple solutions of chromatographers. Hydrogeochemists face even greater problems than soil scientists, as they have few sampling points, lack analyses of the solid material, and have not much knowledge of the flowpath and residence time of their water sample in the subsoil. The lack of material information has probably stimulated even more the search for concepts which can explain the observed response of the subsoil to water quality changes during artificial recharge. The foremost chemical process in these transient systems is multicomponent chromatography.

Multicomponent ion exchange is the basis of chromatography. It involves the competition of *all* the ions in pore water for the soil exchanger(s). Because natural exchangers show different selectivity for different cations, the ratio of sorbed over solute concentration is variable for individual cations. This implies that retardation (or transport velocity) is different for different species, and that transport will induce separation of solutes according to individual transport velocities. By definition chromatography uses this behavior in a laboratory column to separate components from a complex mixture.

The pioneering studies on multicomponent chromatography of Sillén (1951), of Klein, Tondeur and Vermeulen at the seawater conversion laboratory (Klein et al., 1967), and of Helfferich and Klein (1970), form the basis for a quantitative description. The theory was rapidly investigated for application to enhanced oil recovery (Pope et al., 1978; DeZabala et al., 1982). Numerical modeling of subsoil transport was almost immediately combined with multicomponent exchange formulations (Rubin and James, 1973; Valocchi et al., 1981a, b; and many others more recently, cf. Yeh and Tripathi, 1989, and Mangold and Tsang, 1991). Hydrochemists have at an early stage recognized that $NaHCO_3$ waters in coastal areas are connected with cation exchange (Foster, 1950; Back, 1966; Chapelle and Knobel, 1983). It may be that the analytical tools of the chromatographers were somewhat neglected as numerical models were applied very directly to subsoil transport problems.

0275-0279/96/0034-0004$05.00

However, the chromatographic concepts are also appearing in the hydrogeological literature (Schweich and Sardin, 1981; Charbeneau, 1981; 1988; Appelo et al., 1993, 1994b; Schweich et al., 1993).

The purpose of this chapter is to show how decisive the role of multicomponent cation exchange in hydrochemistry can be and to illustrate chromatographic concepts with practical examples. Applications so far have been mainly related to man-induced effects in aquifers such as artificial recharge or injection tests. However, examples of natural water qualities that are the result of chromatography are now also available (Beekman, 1991; Manzano et al., 1992; Stuyfzand, 1993; Appelo, 1994a; Walraevens and Cardenal, 1994; Hansen and Postma, 1995). The intricacies of nature require calculations with numerical models to be able to *match* what is observed. On the other hand, having chromatographic concepts and simple tools helps us to gain a fundamental understanding of the processes involved. It may also help us to recognize the broader applicability of this field in geochemistry.

The chapter begins with the basic equations to calculate multicomponent equilibria and shows that calculating these equilibria is meaningful. Much of the chromatographic theory is related to front type and front development, and this is treated for one component. The concepts are illustrated with column experiments from the literature or compared with numerical model results. Then multicomponent chromatography is considered, in the sense of having a system of linear equations that can be solved by the method of characteristics, or similar, recently developed mathematical tools. Examples from the hydrochemical literature demonstrate applicability.

EXCHANGE EQUILIBRIA AND CALCULATIONS

Soil chemical laboratories express cation exchange capacity (*CEC*) of soils in meq/100g (dry) sample. To obtain meq/l pore water, the *CEC* is multiplied with 10 times the bulk density ($10 \times \rho_b$, g/cm^3) to give meq/dm^3 sediment, and then divided by the water filled porosity (ε, -). A *CEC* of 1 meq/100g, which is representative for a fine sand, amounts to 60 meq/l pore water with $\rho_b = 1.8$ g/cm^3 and $\varepsilon = 0.3$. The pool of exchangeable cations is therefore quite high compared to concentrations in fresh water. Figure 1 shows amounts of exchangeable cations and total cation concentrations in fresh water and in seawater, and illustrates the relative proportions.

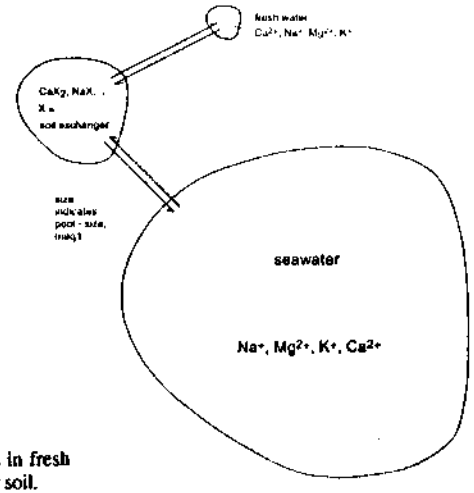

Figure 1. Comparison of solute concentrations in fresh water and seawater, and exchangeable on a sandy soil.

Also indicated in Figure 1 is the multicomponent character of ion exchange. The cations are in mutual competition for the exchanger sites, and the ratio of sorbed over solute concentration (the distribution coefficient K_d, -) increases with increasing selectivity. The distribution coefficient is a variable for the individual solutes, which moreover depends on the solution composition. Thus, for seawater in a fine sand, $K_d \approx 0.06$ for Na^+, while $K_d \approx 600$ for protons. In fresh water with 3 mmol/l Ca^{2+} and 1 mmol/l Na^+, $K_d \approx 0.3$ for Na^+, and at pH = 7.0, $K_d \approx 90{,}000$ for protons. The distribution coefficients were calculated from multicomponent exchanger compositions, in equilibrium with the aqueous solution. These exchanger compositions are often calculated with Newton iteration from aqueous concentrations, but analytical solution is possible by suitable rearrangement of the equations as will be shown in the following section.

Exchange equations

Equilibrium among solute and exchangeable cations is calculated with the law of mass action. For example, for Na^+ and K^+ the reaction is

$$Na^+ + K\text{-}X \leftrightarrow Na\text{-}X + K^+ \tag{1}$$

The law of mass action relates the activities as

$$K_{NaK} = \frac{[Na\text{-}X]\,[K^+]}{[K\text{-}X]\,[Na^+]} \tag{2}$$

The brackets indicate activities. For the solute ions these are a fraction of the standard state of 1 mol/kg H_2O (thus, numerically almost equal to the concentration in mol/l). For the exchangeable cations the equivalent fraction is used (Gaines and Thomas, 1953). Activity coefficients and complexation in solution and in the exchanger are neglected when in this chapter approximate solutions are calculated; they are included in the results from numerical models that are presented for comparison. The equivalent fraction $\beta_i = [i\text{-}X_{z_i}]$ of an exchangeable cation is calculated from measured concentrations and *CEC*. For example, when *CEC* = 1.2 meq/100g, and Na-X = 0.3 meq/100g, $\beta_{Na} = 0.25$. Because activity coefficients equal to 1 are assumed, $[Na\text{-}X] = \beta_{Na} = 0.25$. We also have the sum

$$\Sigma \beta = 1 \tag{3}$$

In general for two cations $i_{z_i}^+$ and $j_{z_j}^+$ the exchange equation is:

$$1/z_i\, i_{z_i}^+ + 1/z_j\, j\text{-}X_{z_j} \leftrightarrow 1/z_i\, i\text{-}X_{z_i} + 1/z_j\, j_{z_j}^+ \tag{4}$$

with

$$K_{ij} = \frac{\beta_i^{1/z_i}\,[j^{z_j+}]^{1/z_j}}{\beta_j^{1/z_j}\,[i^{z_i+}]^{1/z_i}} \tag{5}$$

This equation, together with (3), allows all β's to be determined in a multicomponent solution when the aqueous concentrations are known. To this end, β_j of ion $j_{z_j}^+$ is expressed as a function of β_i:

$$\beta_j = \frac{[j^{z_j+}]}{K_{ij}^{z_j}\,[i^{z_i+}]^{z_j/z_i}}\,\beta_i^{z_j/z_i} \tag{6}$$

Thus, β_k ..... of ions $k z_k^+$,.... are all expressed as function of β_i . All β's are entered in the sum

$$\beta_i + \beta_j + \beta_k + \ldots = 1 \tag{3a}$$

to give an equation with only β_i as the unknown. It is convenient to use a monovalent ion (Na^+) as the reference cation $i z_i^+$, because that gives a quadratic equation for the system with Na^+, K^+, Mg^{2+} and Ca^{2+} (mono- and divalent ions in general). Equation (3a) can be solved to give one positive root for β_{Na}. Subsequently the other β's are obtained from (6).

The other option—calculating the solution from known exchanger composition—follows in the same way, but now the sum of the cations in solution is the equation to solve:

$$\Sigma z_i c_i = N \tag{7}$$

where c_i is the concentration of i (mol/l), and N is the normality of the solution (eq/l). Again, it is advantageous to express all concentrations as function of a monovalent ion (Na^+) as it leads immediately to a quadratic (or cubic when trivalent ions are present) equation with one unknown. Example calculations can be found in Appelo and Postma (1993) and Appelo (1994b).

A particular effect of exchange equilibrium is observed if salinity changes. When exchangeable cations form a large pool that buffers the solution composition, the ratios of solute concentrations are fixed as

$$\frac{[j^{z_j+}]^{1/z_j}}{[i^{z_i+}]^{1/z_i}} = K_{ij} \frac{\beta_j^{1/z_j}}{\beta_i^{1/z_i}} \tag{5a}$$

A 10-fold change of the Na^+ concentration is accompanied by a 100-fold change of the Ca^{2+} concentration and a 1000-fold change of the Al^{3+} concentration. Dilution gives a relative increase of monovalent cations, salinity increase leads to a relative increase of polyvalent cations.

Values for the exchange coefficients K_{NaV} are listed in Table 1. A range is indicated because they depend somewhat on the soil mineral and the solution composition (Bruggenwert and Kamphorst, 1982). This is implicit to the fact that different exchange sites exist on the minerals and that activity coefficients for the exchangeable cations are assumed to be 1.

The coefficient for other exchange reactions between ions $i z_i^+$ and $j z_j^+$ can be calculated conveniently from the values in Table 1 with

$$K_{ij} = K_{iNa} \cdot K_{NaV} \tag{8}$$

Also, it is obvious that

$$K_{iNa} = \frac{1}{K_{NaV}} \tag{9}$$

In geochemical computer models that use ion association, the exchange reaction can be calculated by splitting the exchange reaction into two association reactions of the cations with X^- (Parkhurst, 1995). A reference reaction reaction has to be specified, and all the other coefficients then follow. For example, when the reference reaction is for Na-X:

Table 1. Values for exchange coefficients with respect to Na^+ (Gaines-Thomas-convention, i.e. equivalent fraction is used for exchangeable cations). From Appelo and Postma, 1993.

Equation: $Na^+ + 1/z_i\, i\text{-}X_{z_i} \leftrightarrow Na\text{-}X + 1/z_i\, i^{z_i+}$

$$K_{NaV} = \frac{[Na\text{-}X]\,[i^{z_i+}]^{1/z_i}}{[i\text{-}X_{z_i}]^{1/z_i}\,[Na^+]} = \frac{\beta_{Na}\,[i^{z_i+}]^{1/z_i}}{\beta_i^{1/z_i}\,[Na^+]}$$

Ion i^+	K_{NaV}	Ion i^{2+}	K_{NaV}	Ion i^{3+}	K_{NaV}
Li^+	1.2 (0.95-1.2)	Mg^{2+}	0.50 (0.4-0.6)	Al^{3+}	0.6 (0.5-0.9)
K^+	0.20 (0.05-0.25)	Ca^{2+}	0.40 (0.3-0.6)	Fe^{3+}	?
NH_4^+	0.25 (0.2 -0.3)	Sr^{2+}	0.35 (0.3-0.6)		
Rb^+	0.10	Ba^{2+}	0.35 (0.2-0.5)		
Cs^+	0.08	Mn^{2+}	0.55		
		Fe^{2+}	0.6		
		Co^{2+}	0.6		
		Ni^{2+}	0.5		
		Cu^{2+}	0.5		
		Zn^{2+}	0.4 (0.3-0.6)		
		Cd^{2+}	0.4 (0.3-0.6)		
		Pb^{2+}	0.3		

$$Na^+ + X^- \leftrightarrow Na\text{-}X\,; \quad \log K = 0.0 \tag{10}$$

then for the other cations the reaction is

$$1/z_i\, i^{z_i+} + X^- \leftrightarrow 1/z_i\, i\text{-}X_{z_i}\,; \quad \log K = \log K_{iNa} = -\log K_{NaV} \tag{11}$$

A problem may arise when the concentration of X^- is a variable, e.g. when X^- is made proportional to a solid that may dissolve *or* precipitate, or because a mineral has a variable charge that depends on solution composition (cf. Lichtner's chapter). Charge in the aqueous solution appears no longer to be conserved because the solution loses cations if X^- increases and gains them if X^- decreases. Charge of the aqueous solution is used in geochemical models to calculate the concentration of a component (often pH), and a computation that neglects these effects may go wrong completely. However, charge must be conserved for the combination of mobile and immobile entities of the model system. An increase of immobile charge X^-, can only be due to an equivalent loss of negative charge from solution. Because the increased X^- is compensated by positive counterions that are also derived from solution, the charge transfer is balanced. A similar reasoning holds when X^- decreases. The total charge of either the mobile or the immobile part, therefore, remains equal.

Parkhurst (1995) has solved the problem of variable charge and charge transfer among solid and solution in PHREEQC by calculating explicitly the double layer counter- and co-ions that compensate the variable charge. The double layer charge is assigned to the immobile mineral to form a unit which remains electrically neutral. Similarly, when charge is associated to a specific mineral that precipitates or dissolves, an exchange model can be constructed in which only neutral molecules can be adsorbed (Appelo et al., 1996).

Determination of exchangeable cations

Much of the acceptance of chromatographic theory for soils and aquifers rests on experimental proof that exchangeable cations correspond to the calculated equilibria. Exchangeable cations are routinely analyzed by displacement with a solution that is free of the cations of interest (Page et al., 1982). The difficulty lies in separating the exchanged cations from the contribution by the soil solution and from the reactions that occur when an extractant is applied to the sediment sample.

The contribution of pore water can be high for Na^+, which often has a low distribution coefficient. Pore water contributions are sometimes reduced by displacing the pore solution with alcohol, where it is assumed that the exchangeable cations are not affected. (Note that rinsing with water is strictly taboo, since a dilution of the equilibrium solution displaces the lower charged ions from the exchange complex, cf. Eqn. 5). The influence can also be reduced by centrifuging the pore water.

Bothersome side reactions are dissolution of salts (notably gypsum) and carbonates, and oxidation of minerals (pyrite) in case of a reduced sediment. The latter reaction can be prevented by working under anaerobic conditions. Dissolution of minerals is corrected by analyzing SO_4^{2-} and HCO_3^- in the extract, and subtracting the anion concentrations from Ca^{2+} and, in case dolomite is present, from Mg^{2+}. Obviously, the displacing cation must not precipitate with this anion, which precludes use of the divalent cations Sr^{2+} and Ba^{2+}.

Monovalent ions are therefore preferred as displacers. A high concentration of at least 1M is necessary for displacement of divalent and trivalent ions, which puts a claim on purity. Ammonium and the heavier alkaline ions increase proton exchange and carbonate dissolution. It makes the HCO_3^- correction on Ca^{2+} more difficult because part of alkalinity is compensated by protons. Lithium is not commercially available in pure enough form to analyze Na^+, and it very readily peptizes clay and organic matter. Na^+ is therefore the obvious choice for displacing exchangeable cations. Exchangeable Na-X can be displaced with NH_4Cl. The technique using 1M NaCl and 1M NH_4Cl for analyzing exchangeable cations was developed by Zuur (1938), cited by Van der Molen (1958). It has been applied by Van der Molen (1958), and in studies related to poldering in The Netherlands (Hofstee, 1971). [Poldering is the reclamation of low-lying land from sea or river, practiced in the Netherlands.] We have found that it is the only rapid (batch) method that gives exchange coefficients for a large variation of aqueous solutions and aquifer sediments that are consistent with those in Table 1 (cf. Appelo et al., 1996).

For example, Van der Molen (1958) has determined exchangeable cations in two soils equilibrated with mixtures of seawater and distilled water. His results for two soils are compared in Figure 2 with model calculations using the log K_{IX} for the association reaction given in Table 2. To obtain a good fit of observed fractions over the full range from fresh water to seawater, the selectivity for Na^+ has to decrease by 0.5 log-units when going from fresh water to seawater. The selectivity coefficient for fresh water yields $\beta_{Na} = 0.6$ for seawater, whereas experimentally $\beta_{Na} \approx 0.4$.

As another example, exchangeable cations in young soils that were poldered from the sea are plotted as a function of seawater fraction in Figure 3 (Groen, 1991). Only Cl^- was analyzed in the soil solution, and the other ions were estimated assuming that the soil solution was a mixture of seawater and 3 mM $Ca(HCO_3)_2$ water. The seawater fraction was based on Cl^- concentration. Thick lines are model exchange compositions using the coefficients from Table 2. Thin, dotted lines give compositions when the coefficients from

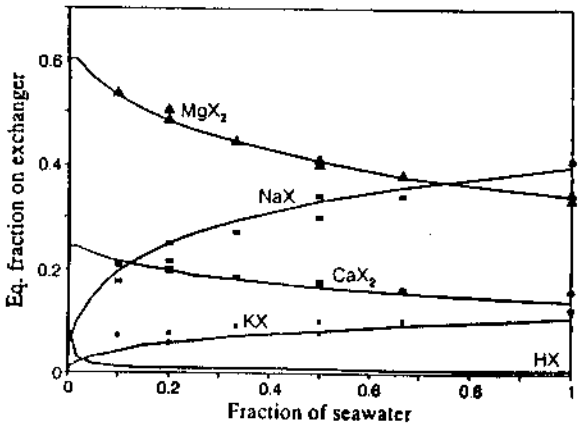

Figure 2. Fractions of exchangeable cations on two soils in mixtures of seawater and distilled water. Analyzed fractions indicated by single points; lines are modeled concentrations with exchange coefficients from Table 2. [Used by permission of the editor of *Water Resources Res.*, from Appelo (1994)].

Table 2. Association coefficients for the reaction $1/z_i\ i\text{-}X_{z_i} + X^- \leftrightarrow 1/z_i\ i\text{-}X_{z_i}$ in Van der Molen's exchange experiment with fresh water and seawater (Appelo, 1994a).

	Na^+	K^+	Mg^{2+}	Ca^{2+}
log K_{IX}	$-0.5+0.5(1-\beta_{Na})$	0.902	0.307	0.465

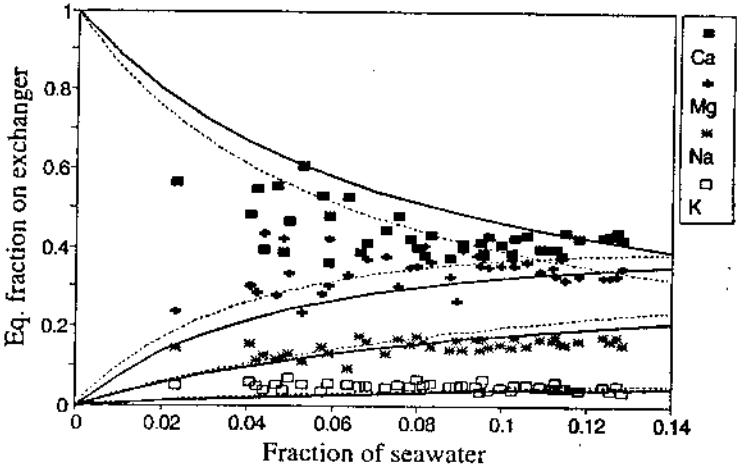

Figure 3. Fractions of exchangeable cations in polder soils as function of Cl^- concentration (seawater fraction) in the soil solution. Analyzed fractions from Groen (1991). Model lines: thick lines with variable selectivity for Na^+ (exchange coefficients from Table 2), dotted lines with 'standard' exchange coefficients (from Table 1).

Table 1 are used. The selectivity for K^+ has been increased by decreasing $K_{Na\backslash K}$ to 0.1, as it fits better for the illitic Dutch soils. There is clearly a large spread among the determined values, and the lines only indicate the trends in these values. On the other hand, doing a calculation with an estimated soil solution composition which is not far wrong, shows that the basic theory of multicomponent exchange calculations is correct.

One may speculate why the multicomponent exchange equilibria work so well, while it should not be doubted that precise measurements on individual exchangers necessitate use of activity coefficients (Elprince and Babcock, 1975; Bichkova and Soldatov, 1985; Franklin and Townsend, 1988; Sposito, 1994). It certainly can not be explained with double layer theory. The apparent selectivity, calculated from excess Na^+/Ca^{2+} in the double layer, is about equal to the values in Table 1 when the solution has seawater normality (Bolt, 1967). However, a dilution has not much effect on the ratio of mono- and divalent ions in the double layer. The apparent selectivity (log $K_{Na\backslash Ca}$) therefore increases markedly upon dilution; this in contrast to observations as in Figures 2 and 3.

CHROMATOGRAPHIC PATTERNS

With functional equilibrium relations among solute and sorbed cations, the effect of water quality changes must be considered. This is studied under the heading of ion-chromatography in chemistry and chemical engineering (DeVault, 1943; Sillén, 1951; Glückauf, 1955; Tondeur, 1969; Helfferich and Klein, 1970; Vermeulen et al., 1984; Rhee et al., 1989). The theory has been applied and verified in numerous laboratory experiments with a variety of soils and sediments (Pope et al., 1978; DeZabala et al., 1982; Schweich et al., 1983; Rainwater et al., 1987; Beekman and Appelo, 1990; Appelo et al., 1990; Bond and Phillips, 1990; Griffioen et al., 1992; Bürgisser et al., 1993; Cernik et al., 1994; Scheidegger et al., 1994). A chromatographic origin has been recognized for water quality changes during well injections (Valocchi et al., 1981a,b; Charbeneau, 1988; Bjerg et al., 1993). Also with large scale freshening of saline aquifers, a sequence of water qualities develops along a flow path that can be related to multicomponent cation exchange (Appelo and Willemsen, 1987; Beekman, 1991; Stuyfzand, 1993; Appelo, 1994a; Walraevens and Cardenal, 1994). It is clear that the theory can be applied in hydrogeology, and that it deserves attention as an important basic process for regulating water quality in aquifers.

The following parts of this chapter illustrate the development of chromatographic patterns, and show how to calculate them in a simple way and compare these also with numerical models. First, the basic equations for single solute transport are presented and illustrated. The shape of the sorption or exchange isotherm is of fundamental importance for solute transport and determines the front type along a flowline and during passage along an observation well. This also holds for multicomponent transport, but here the equations rapidly become complex. Recourse to numerical models is then appropriate, also because more complex boundary conditions and other chemical processes can be included.

Single solute transport, broadening fronts

The advection-dispersion-reaction equation in one dimension gives the change in concentration with time for a solute species:

$$\frac{\partial c}{\partial t} = -v\frac{\partial c}{\partial x} + D\frac{\partial^2 c}{\partial x^2} - \frac{\partial q}{\partial t} \qquad (12)$$

where c is concentration in solution (mol/l), t is time (s), v is pore water flow velocity (m/s), x is distance (m), D is the dispersion coefficient (m^2/s), and q is the sorbed concentration, expressed as a pore water concentration (mol/l). In the case of ion exchange, $q_i = \beta_i \cdot CEC \cdot 10\rho_b/\varepsilon$ as was noted before.

Analytical solutions can be obtained for varying q/c, but the dispersion coefficient D must be assumed zero. This is what we shall pursue here, because we already concluded that with multicomponent exchange $K_d = q/c$ for the individual elements is variable.

With $D = 0$ and the slope of the isotherm dq/dc, Equation (12) becomes:

$$\left(1 + \frac{dq}{dc}\right)\frac{\partial c}{\partial t} + v\frac{\partial c}{\partial x} = 0 \qquad (13)$$

A constant concentration means $dc = 0$, and therefore:

$$dc = \left(\frac{\partial c}{\partial t}\right)dt + \left(\frac{\partial c}{\partial x}\right)dx = 0 \qquad (14)$$

or

$$\left(\frac{\partial x}{\partial t}\right)_c = -\left(\frac{\partial c}{\partial t}\right)\left(\frac{\partial x}{\partial c}\right) \qquad (15)$$

On combining with Equation (13), v_c, or the velocity of a constant concentration c, is obtained as

$$v_c = \frac{v_{H_2O}}{1 + \frac{dq}{dc}} \qquad (16)$$

for clarity the pore water flow velocity is indicated as v_{H_2O}. Equation (16) is similar to the retardation equation in that it shows that the velocity of a solute is retarded due to sorption. However, the velocity is now variable for different concentrations and depends on the slope dq/dc.

The distance x traveled by a retarded solute c_i can be simply calculated and compared with that traveled by a conservative solute c_a (which has $dq_a/dc_a = 0$). In both cases we have $x = v\,t$, and therefore

$$x_{c_i} = \frac{x_{c_a}}{1 + \frac{dq_i}{dc_i}} \qquad (17)$$

Figure 4 illustrates front development for a conservative solute a, and solutes i and j whichhave $q_i = c_i$ ($R = 2$) and $q_j = \sqrt{c_j}$ ($R = 1 + 1/2\sqrt{c}$). The initial concentration of all solutes is 1 at all x, and water enters at $x = 0$ with $c_i = c_j = c_a = 0$. Substance a has been flushed till 70 m, the location of the advective front. The position of 2 concentrations of each of the three substances is given in Table 3. Flushing of i is retarded, the concentration

drops to zero at $x = 70/(1 + 1) = 35$ m. Flushing of j starts earlier than of i, the concentration begins to decrease at $x = 70/(1 + 0.5) = 46.7$ m. Smaller concentrations travel slower as the slope dq/dc increases in accordance with Equation (17), and these concentrations have moved less. Chemicals a and i show *indifferent* fronts, meaning that all concentrations have identical velocity. Chemical j shows a *broadening* or *diffuse* front upon elution, also called a *wave* or a *simple wave*.

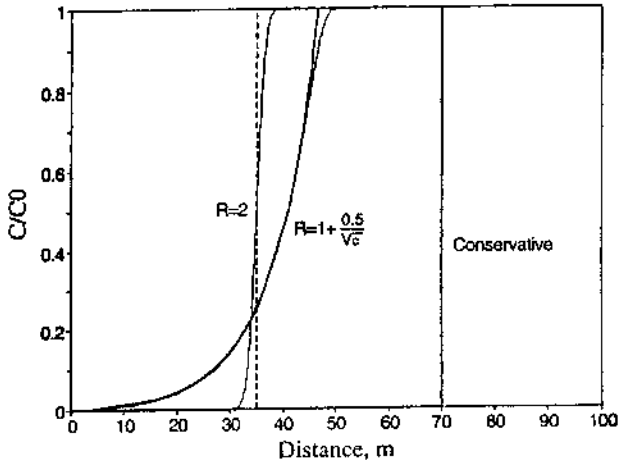

Figure 4. Flushing of a conservative chemical ($q_a = 0$ for all c_a), a linearly sorbed chemical with $R = 2$ ($q_i = c_i$), and a chemical with variable R ($q_j = \sqrt{c_j}$). The initial condition is $c = 1$ for all x, and $c = 0$ at $x = 0$, $t > 0$. Thin lines are from numerical model with $\Delta x = 0.1$ m.

Table 3. Example calculations for the position of two concentrations of three substances with different isotherms during flushing along a flowline.

c	$q_a = 0$ ($dq/dc=0$)	$q_i = c_i$ ($dq/dc=1.0$)	$q_j = c_j^{1/2}$ ($dq/dc = 0.5c^{-1/2}$)
1.0	70	35	46.7
0.5	70	35	41.0

Results of a finite difference model are given for i and j with flux boundary conditions at $x = 0$ and $dc/dx = 0$ at $x = \infty$ (cf. example 9.14 in Appelo and Postma, 1993). The concentration of j starts to decrease in a singular point (the derivative dc/dx is not defined). It can be seen that the numerical model shows dispersion around this point where c_j starts to fall. The rest of the c_j profile is correctly followed.

Equation (17) also gives a fairly good approximation in case dispersion is present, at least when its effect is overruled by chemical dispersion (Bolt, 1982). Figure 5 shows the same case as Figure 4, with additional dispersivity $\alpha = 3.3$ m. The numerical model is now more correct as it uses the numerical dispersion to mimick part of the physical dispersion (cf. Appelo and Postma, 1993). The analytical solution of Lindstrom et al. (1967) is plotted for $R = 2$, but it is indiscernible from the numerical model in Figure 5. The approximation

for $R = 2$ by Equation (17) is incorrect as it assumes that dispersion increases linearly with x (dispersion increases with $\sqrt{x}$).

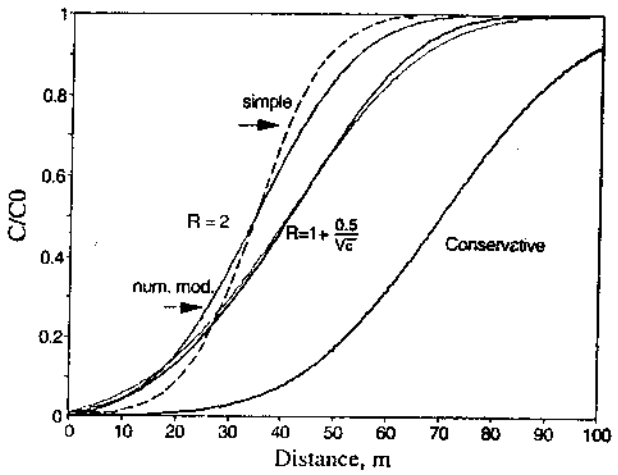

Figure 5. Flushing of two chemicals as in Figure 4, but with dispersion. Dispersivity $\alpha = 3.3$ m. Thin lines are from numerical model ($\Delta x = 0.5$ m) and from the Lindstrom et al. (1967) analytical solution for $R = 2$. Note that the simple approximation with Equation (17) for $R = 2$ is incorrect.

Sharp fronts

When chemical j (with $q_j = \sqrt{c_j}$) enters a pristine aquifer, then again, small concentrations advance more slowly than high concentrations. This would mean that the higher concentrations of j would arrive earlier at some point than the small concentrations. This is clearly impossible. Rather, the high concentrations push up the smaller concentrations, and all concentrations arrive simultaneously. Such arrivals are evocatively denoted as *self-sharpening* fronts, or *shocks*. They form the basis for *displacement* chromatography.

The front position can be calculated from the integral mass balance:

$$\Delta c \cdot (x_{H_2O} - x_j) = \Delta q \cdot x_j \qquad (18)$$

where x_{H_2O} is the position of the conservative front, and x_j the position of the sharp front for j. Δc and Δq are the changes in respectively the solute and sorbed concentrations over the front. With $x = v\,t$ the velocity of the front is obtained as in Equation (16):

$$v_c = \frac{v_{H_2O}}{1 + \dfrac{\Delta q}{\Delta c}} \qquad (19)$$

Figure 6 illustrates the fronts for chemical a and two concentrations of j along the 100 m flowline. The calculations for the front positions are given in Table 4. Note how the front for $c_j = 0.2$ ($R = 3.2$) is retarded more than for $c_j = 1.0$ ($R = 2$). Once more results of the numerical model are shown for comparison, but now the chemical term helps in counteracting numerical dispersion. The numerical model therefore almost coincides with the sharp front approximation.

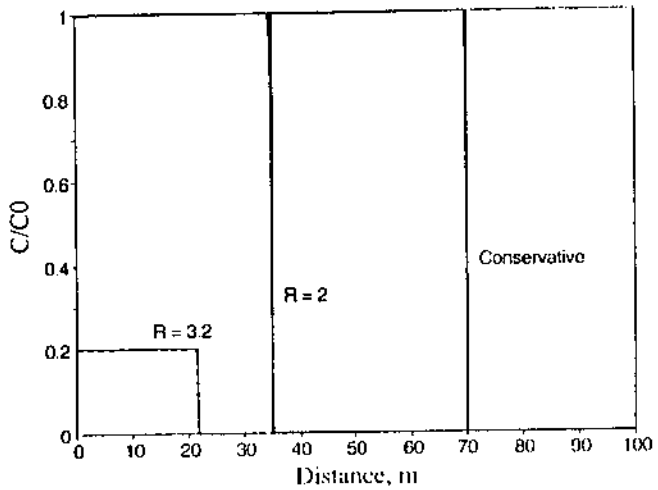

Figure 6. Transport of the chemical *j* from Figure 4 ($qj = \sqrt{cj}$). in a clean flowtube at two concentrations. Note the different retardations that follow from different $\Delta q/\Delta c$ at the two concentrations. Thin lines from numerical model ($\Delta x = 0.5$ m) almost coincide with the sharp front solution.

Table 4. Sharp front positions for two concentrations of substance j which has ($qj = \sqrt{cj}$).

c	x_{H_2O}	q	$\Delta q/\Delta c$	R	x_j	dq/dc
0.2	70	0.44	2.24	3.24	47.9	1.18
1.0	70	1.0	1.0	2	61.5	0.5

Two-cation exchange

With exchange, q is expressed as fraction β of *CEC*, as noted before. For a system with two cations, only one equation [(16) or (19)] suffices because the other cation is automatically obtained as the complement. Bond and Phillips (1990) have measured concentration profiles with Na^+ or K^+ displacing Ca^{2+} in an unsaturated soil column during unsteady flow infiltration. The exchange isotherms for the two ions are given in Figure 7.

The exchange isotherm for Na^+ is concave at all concentrations, hence small concentrations have higher velocity than high concentrations. For Na^+ entering the soil column, a broadening front results. For K^+ the exchange isotherm at 0.2N shows a selectivity reversal that Mansell et al. (1993) have modeled using an additional exponent for the solute concentration ratio. The isotherm has a convex part at low K^+ concentrations, and a concave part at high concentrations. Small concentrations will therefore give a sharp front. However, because with increasing K^+ concentrations the slope of the isotherm increases again, the high concentrations are retarded more, thus leading to a broadening front for the highest concentrations. The turnover point lies where the isotherm slope is equal to the slope at $K^+ = 0$.

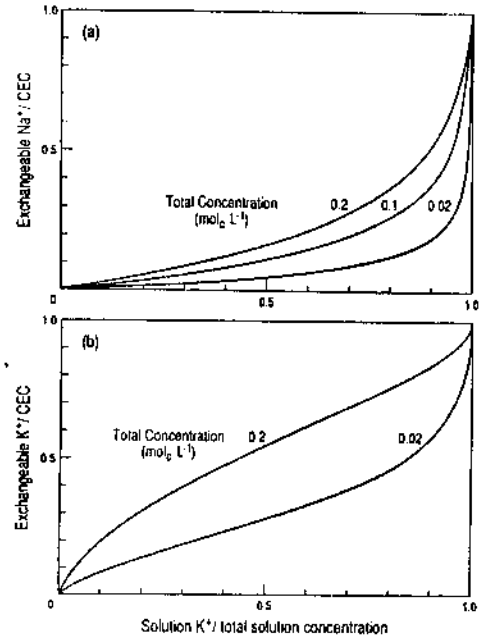

Figure 7. Exchange isotherms for (a) Na-Ca exchange and (b) K-Ca exchange at different normality N (indicated as $mol_c\ L^{-1}$) [Used by permission of the editor of *Water Resources Res.*, from Bond and Phillips (1990)].

The calculations for the two cases are somewhat elaborate because the exchange is among heterovalent ions, and because flow is unsteady. However, the above procedure of relating retardation of concentrations to isotherm slope has been used by Bond and Phillips (1990) to calculate concentrations profiles. These are compared with experimental data in Figure 8. Very clear is the fact that the Na^+ profile is broadening, while the K^+ front is sharp over a large domain and broadening for the highest concentrations only.

Column elution curves

It is equally simple to calculate elution curves for a column. The relative arrival time t/t_0 is calculated at fixed $x = L$, the end of column, with Equation (16):

$$t/t_0 = 1 + dq/dc \tag{20}$$

where t_0 is the time used by a conservative substance to pass through the column. The ratio t/t_0 is known as the *throughput ratio* (Vermeulen et al., 1984). It can also be expressed as relative volumes V/V_0, where V_0 is the pore volume of the column. If Equation (20) is condensed to just the slope of the isotherm, it indicates the pore volumes that are needed *after* the conservative front has passed. It has been termed the ψ condition (Sillén, 1951), or the *flushing factor* V^* (Appelo and Postma, 1993):

$$V^* = V/V_0 - 1 = dq/dc \tag{21}$$

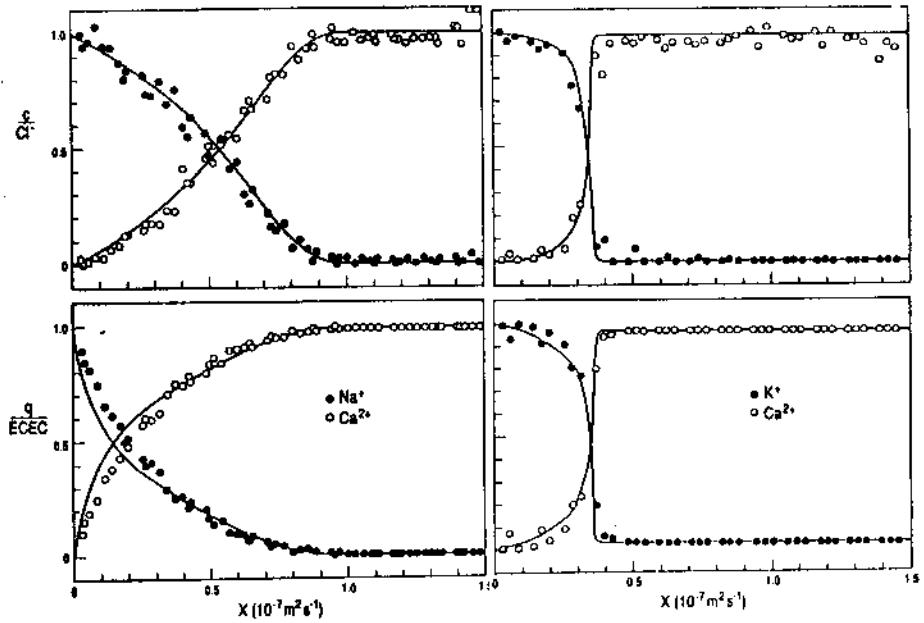

Figure 8. Comparison of measured (symbols) and modeled (lines) distributions of solution and sorbed cation concentrations following the entry of 0.2 mol/l solution of NaCl (left) and KCl (right). The X axis is a normalized distance that includes the varying flux in the unsaturated column (the columns are between 0.2 and 0.35 cm in length). The cation concentrations are normalized to total anion concentration and *CEC*. [Used by permission of the editor *Water Resources Res.*, from Bond and Phillips (1990)].

The equation is for broadening fronts, when the slope of the isotherm is smaller at the initial condition of the column than at the end. If the slope of the isotherm *decreases* towards the final condition, the final condition pushes the earlier compositions forward, and a sharp front results. The integral mass balance applies again, and a *sharp front flushing factor* is defined as:

$$V^* = \Delta q/\Delta c \tag{22}$$

Column elution curves are qualitatively pictured in Figure 9.

Sorption isotherms from elution curves

The sorption isotherm can be deduced from a measured elution curve by integration of Equation (21). For sharp fronts obviously only one point of the isotherm is obtained. For broadening fronts the whole isotherm over the range from start to final concentration can be derived (Glückauf, 1945; Sillén, 1950) For a broadening elution curve the change of q from c_1 to c_2 is:

$$q_2 - q_1 = \int_{q_1}^{q_2} dq = \int_{c_1}^{c_2} V^* \, dc \tag{23}$$

Thus from a starting condition with known q_1, q_2 can be obtained by integrating the elution curve. The procedure is illustrated in Figure 10. Note that the integration is along the vertical axis from c_1 to c_2. Also note that the integration gives a negative number when performed from c_1 (high) to c_2 (low), which agrees to the negative sum $q_2 - q_1$.

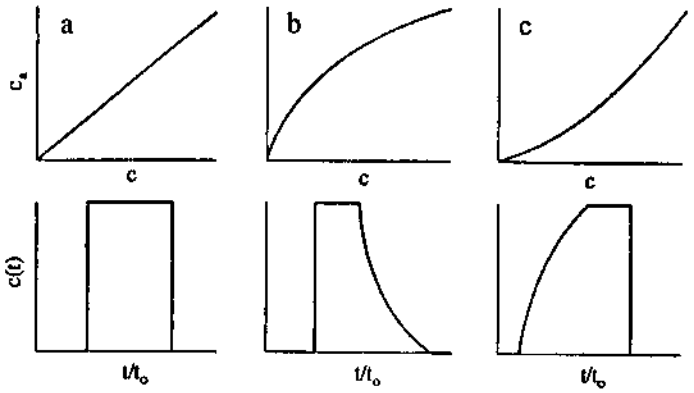

Figure 9. Schematic representation of the response of a column for different sorption isotherms (top). The column breakthrough of a step concentration change without dispersion effects is shown (below) for different isotherms: (a) linear, (b) convex, and (c) concave. [Used by permission of the editor of *Environmental Science and Technology*, from Bürgisser et al. (1993)].

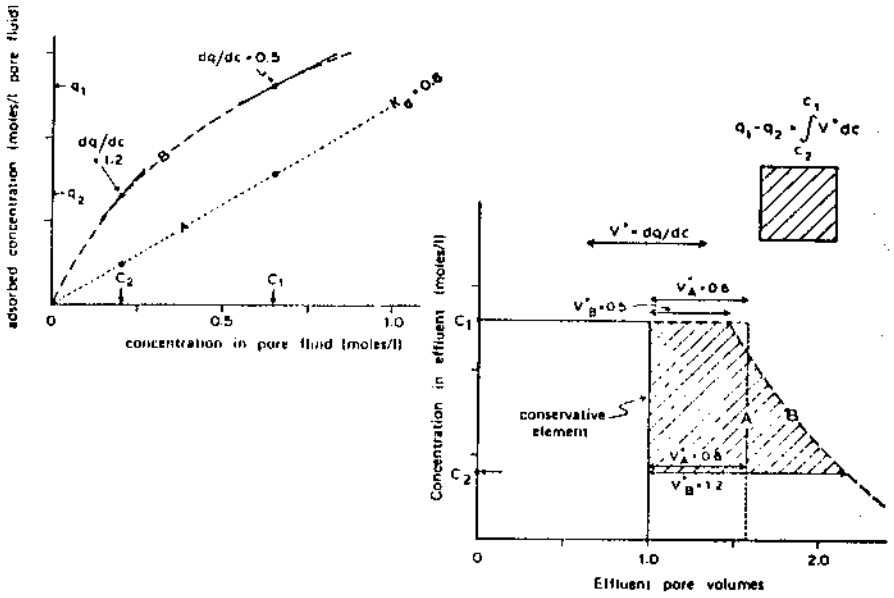

Figure 10. A broadening elution curve can be used to obtain the sorption isotherm, as illustrated for substance B. *Left:* isotherms for A (linear) and B (convex). *Right:* Elution curves for A and B, and integration area to obtain points of the curved isotherm of B. [Used by permission of Balkema, from Appelo and Postma (1993)].

The method was advocated as soon as the character of chromatographic behavior was fully realized (DeVault, 1943; Glückauf, 1945; Sillén, 1950). Several investigators have described the good agreement between sorption isotherms from elution curves and single points obtained from batch experiments (Glückauf, 1949; Duncan and Lister, 1949; Ekedahl et al., 1950; Faucher et al., 1952, 1954; Merriam et al., 1952). However, it was also found that the chromatographic method could be badly in error, and in "complete disagreement with the reliable data from the equilibrium method" (Merriam and Thomas, 1956). Reference to the method in the chemical engineering literature has disappeared since. Clearly, it is not the mathematical description of the process but improper experimentation (too high flow velocity) or incorrect interpretation (neglect of dispersion) that may result in bad data.

In recent years the method has been re-advocated for obtaining sorption or exchange isotherms for natural materials (Schweich et al., 1983; Kool et al., 1989; Griffioen et al., 1992; Bürgisser et al., 1993, 1994; Scheidegger et al., 1994). The principal attraction is that it allows to measure an entire, possibly non-linear isotherm in a one time procedure that takes not much more time than a batch experiment needs for a single point of the isotherm. A column experiment also permits to use a high solid-solution ratio that may be necessary to measure sorption when K_d is very low. Bürgisser et al. (1993) have measured a sorption isotherm of Cd^{2+} on silica sand by the chromatographic method, as shown in Figures 11 and 12. The column experiment has been accomplished at two different flow velocities to show that kinetic effects are absent. The sorption isotherm that was calculated from the elution curve is in very good agreement with results from batch experiments (Fig. 11). With a density of the sand $\rho = 2.31$ g/cm^3 and porosity $\varepsilon = 0.45$, the K_d for Cd^{2+} decreases from approximately 5 to only 0.85 at respectively 1.0 µM and 100 µM Cd^{2+}. Also dq/dc decreases from 4.2 to 0.4 between these two concentrations.

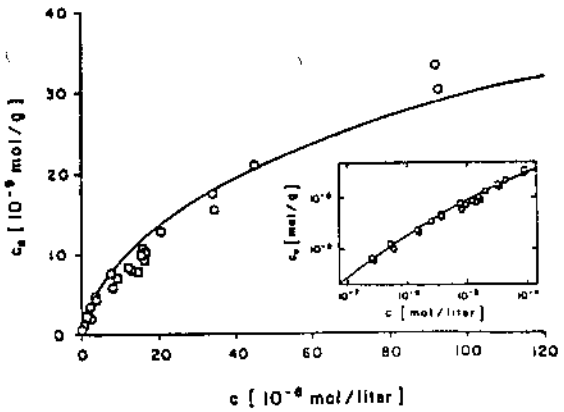

Figure 11. Adsorption isotherm of Cd^{2+} on sand (125 to 250 µm) in 10 mM $NaNO_3$. Symbols from batch experiments, solid line from column elution shown in Figure 12. [Used by permission of the editor of *Environmental Science and Technology*, from Bürgisser et al. (1993)].

Bürgisser et al. analyzed their experiment as a Cd^{2+} sorption process for which the isotherm needs to be found by experimentation. It is illustrative to interpret it as an exchange process of Cd^{2+} for Na^+ from the background electrolyte. The exchange reaction is:

$$Na^+ + 1/2\ Cd\text{-}X_2 \leftrightarrow Na\text{-}X + 1/2\ Cd^{2+} \qquad (24)$$

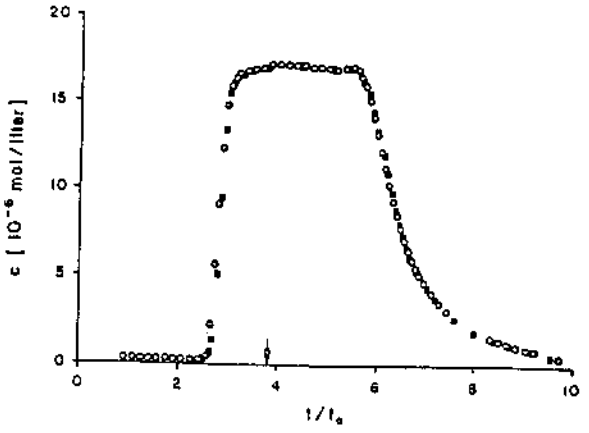

Figure 12. Breakthrough curves of Cd^{2+} in 10 mM $NaNO_3$ from a column packed with sand. Step input of 17.5 µM Cd^{2+} for $0 < t/t_0 < 3.8$. Two symbols are for two different flow velocities. [Used by permission of the editor of *Environmental Science and Technology* from Bürgisser et al. (1993)].

With $K_{Na\backslash Cd} = 0.4$ from Table 1, observed exchangeable Cd^{2+} at 17.5 µM Cd^{2+} is obtained with $CEC = 0.056$ meq/kg sand. The calculated isotherm is shown in Figure 13. It has an initial steep slope that flattens rapidly when concentrations increase above 17.5 µM. Observed exchangeable Cd^{2+} (from batch experiments and from a column experiment with 175 µM Cd^{2+}) is higher. The higher concentrations can be fitted by increasing the CEC to 0.146 meq/l, and increasing $K_{Na\backslash Cd}$ to 0.9 (note the very small exchange capacity of this almost pure cristobalite). This isotherm has a smaller slope at low concentrations that shows more gradual increase towards the higher isotherm points. The small initial slope gives rapid elution of the low concentrations, as is illustrated in Figure 14. Comparison with the observed elution curve suggests that two sorption sites exist on the sand, one with

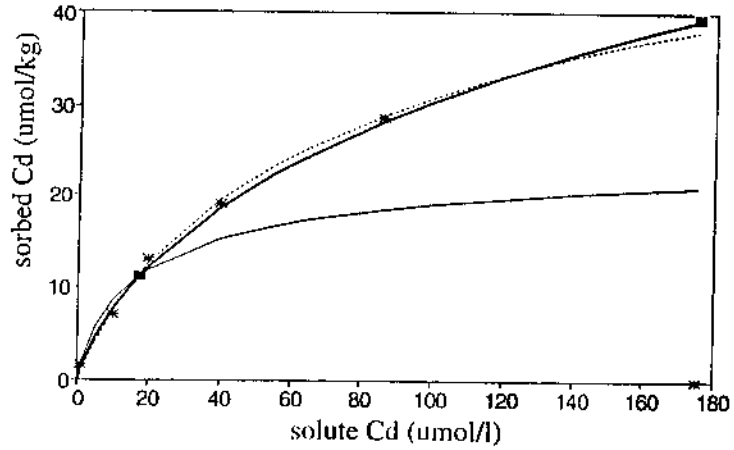

Figure 13. Cd^{2+} sorption on cristobalite sand interpreted as an ion-exchange process against Na^+ from 10mM $NaNO_3$ solution. Filled squares: data from 2 column experiments with sharp fronts; other symbols: batch experiments (Bürgisser et al., 1993). Thin line: $K_{Na\backslash Cd} = 0.4$, $CEC = 0.056$ meq/kg; dotted line: $K_{Na\backslash Cd} = 0.9$, $CEC = 0.146$ meq/kg; thick line: combined isotherm with two selectivity sites (see text).

a standard K that dominates elution of low concentrations < 5 μmol/l, and one with reduced selectivity for Cd^{2+} that determines elution of higher concentrations. The combined isotherm with 0.028 meq/kg standard sites ($K_{Na\backslash Cd}$ = 0.4) and 0.165 meq/kg low sorption sites ($K_{Na\backslash Cd}$ = 1.55) is also shown in Figure 13, and the corresponding elution curve in Figure 14.

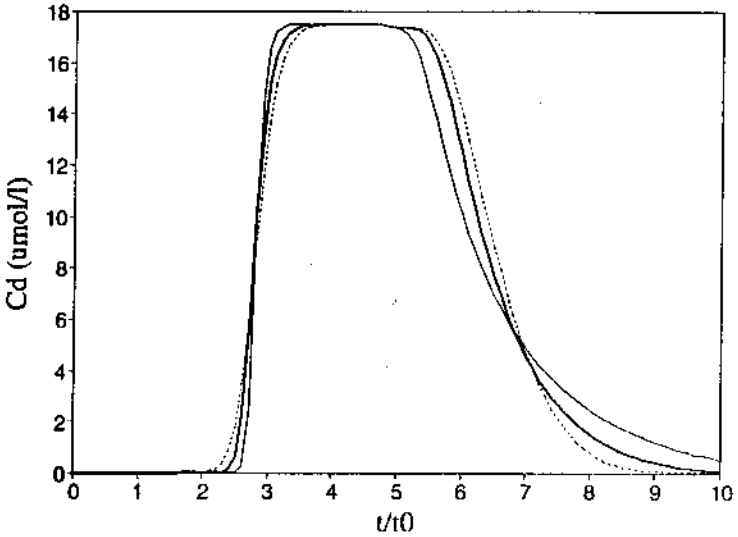

Figure 14. Calculated breakthrough curves for the column experiment of Bürgisser et al. (1993), shown in Figure 12. Three different exchange isotherms have been used, plotted in Figure 13.

The example is of interest as the chromatographic method complements the information from batch experiments. A sound interpretation requires that dispersion is very small (vL/D > 100, as in the example of Bürgisser et al.), or that the elution curve is modeled numerically with a least squares optimization of the adjustable parameters (Kool et al., 1989; Van Veldhuizen et al., 1995).

MULTICOMPONENT CHROMATOGRAPHY

With more than two exchanging cations, the isotherm slope dq/dc for each q_i becomes a variable for all c_j. Still, the mass balance given by Equation (21) for broadening fronts, or by Equation (22) for sharp fronts must hold for each ion. In other words, the flushing factors must be equal for all ions so that in a given solution composition all concentrations have the same velocity. In that case is:

$$V^* = \frac{dq_i}{dc_i} = \frac{dq_j}{dc_j} = ... = \frac{dq_n}{dc_n} \qquad (25)$$

or for a sharp front:

$$V^s = \frac{\Delta q_i}{\Delta c_i} = \frac{\Delta q_j}{\Delta c_j} = ... = \frac{\Delta q_n}{\Delta c_n} \qquad (26)$$

If all ions have to have equal velocity only restricted compositions are possible. When equal velocity exists for all ions according to Equation (25) or (26) the composition is said to be *coherent* (Helfferich and Klein, 1970). The problem is to find these compositions and their succesion when a column in a certain initial condition, is changed by injection of a solution with another composition.

Klein et al. (1967) noted that $V^* + 1$ in Equation (25) is identical to pore volumes eluted. At the corresponding point of the elution curve only dq/dc for the multicomponent solution has to be solved to find c. They have shown that taking the derivative of the log transform of the exchange equilibrium facilitates the problem. Equation (26) can also be solved if only shock fronts occur (Appelo et al., 1993). In both cases the number of roots for V^* or V^s is equal to n-1, where n is the total number of exchanging cations. In case of broadening fronts, these roots are succesively followed from small V^* to large V^*, stepping off when an intermediate composition is reached, and stepping on again when $V^* + 1$ equal the eluted pore volumes. For a system with homovalent cations, the complete sequence can be deduced once and for all by using the H transformation (Helfferich, 1967; Helfferich and Klein, 1970).

Self-similar solution

It is also possible to view the whole system as a Riemann problem and solve it by using the method of characteristics (Tondeur, 1969; Rhee et al., 1970, 1989) or by using the self-similar solution developed by Lax (1957, 1973) and Smoller (1983) as has been done by Charbeneau (1988) and by Thoolen and Hemker (1991). We follow here the treatment by Charbeneau (1988) as it allows for a particularly elegant and quick solution of the system of chromatographic equations.

For a multicomponent system, in which $q_i = f(c_{i,j,...})$, a set of mass balance equations must be solved. Thus, if n species compete for the exchanger sites, (13) becomes:

$$\frac{\partial c_1}{\partial t} + \frac{\partial q_1}{\partial c_1}\frac{\partial c_1}{\partial t} + \frac{\partial q_1}{\partial c_2}\frac{\partial c_2}{\partial t} + ... + \frac{\partial q_1}{\partial c_{n-1}}\frac{\partial c_{n-1}}{\partial t} + v\frac{\partial c_1}{\partial x} = 0$$

$$\vdots \qquad\qquad \vdots \qquad (27)$$

$$\frac{\partial c_{n-1}}{\partial t} + \frac{\partial q_{n-1}}{\partial c_1}\frac{\partial c_1}{\partial t} + \frac{\partial q_{n-1}}{\partial c_2}\frac{\partial c_2}{\partial t} + ... + \frac{\partial q_{n-1}}{\partial c_{n-1}}\frac{\partial c_{n-1}}{\partial t} + v\frac{\partial c_{n-1}}{\partial x} = 0$$

We define $y = x/v$ (the water flow velocity v is steady), and write (27) in matrix form as:

$$(I + Q)\frac{\partial c}{\partial t} + I\frac{\partial c}{\partial y} = 0 \qquad (28)$$

where I is the identity matrix, Q the matrix given by the differential coefficients $(\partial q_i/\partial c_j)_{i,j=1,...,n-1}$, and $\partial c/\partial t$ and $\partial c/\partial y$ are column vectors. The matrix $(I + Q)$ has eigenvalues λ which are found from setting the determinant

$$| I + Q - \lambda I | = 0 \qquad (29)$$

It can be shown that all roots are real and distinct for the multicomponent exchange equations. The roots λ are equal to the flushing factors $V^* + 1$, and thus represent

retardation factors. They may be ordered from $\lambda_1 < \lambda_2 < ... < \lambda_{n-1}$.

The Equations (27) form a quasi linear system of partial differential equations of first order. The initial and boundary conditions which make its solution a Riemann problem are:

$$\begin{aligned} y > 0,\ t = 0\text{: } & c = c^{init},\ q = q^{init} = f(c^{init}) \\ y = 0,\ t > 0\text{: } & c = c^{inj},\ q = q^{inj} = f(c^{inj}) \end{aligned} \tag{30}$$

Now a self-similar variable $\theta = \theta(t/y)$ is defined such that $c = c(\theta)$. It can be used to transform (28) into

$$\left[(I + Q)\frac{\partial\theta}{\partial t} + I\frac{\partial\theta}{\partial y}\right]\frac{dc}{d\theta} = 0 \tag{31}$$

This equation can have only a non-trivial solution if the determinant of the coefficient matrix is zero. The eigenvalues defined by Equation (29) are identical to

$$\lambda = -\frac{\partial\theta/\partial y}{\partial\theta/\partial t} \tag{32}$$

For each eigenvalue, say λ_k, the vector $dc/d\theta$ is a right eigenvector of $(I + Q)$:

$$\frac{dc}{d\theta} = r^k(c) \tag{33}$$

This equation is the essence of the solution of the Riemann problem. Since there are n-1 eigenvalues for $(I + Q)$, there are also n-1 eigenvectors and n-1 intermediate compositions. Each eigenvector represents a part of the compositions that have to be followed from c^{init} to c^{inj} when going in the upstream direction along x. When going from c^{init} in the upstream direction (x decreases), first the eigenvector that belongs to λ_1 is integrated. Along this path, $x_{H_2O}/x = \lambda_1$. When λ_1 of the first intermediate composition is reached, that composition is maintained until $x_{H_2O}/x = \lambda_2$. Then the second eigenvector is taken until λ_2 of the second intermediate composition is reached, etc. The intermediate compositions are called *plateaux*, and the interconnections via the eigenvectors are termed *paths* (Helfferich and Klein, 1970).

The above sequence is valid for broadening waves along the eigenvectors, i.e. λ_k of the k^{th} eigenvector increases upstream. For shock fronts the eigenvalue λ_k that belongs to the $k+1^{th}$ composition is smaller than λ_k of the k^{th} composition. In that case the Rankine-Hugoniot set of Equation (26) must be used.

The general situation for a stepover on the plateau composition or on the following eigenvector is shown in Figure 15. The curved lines are for eigenvectors along which λ increases, and which show gradual composition changes. The straight lines are for shocks, where the composition abruptly changes from the one at the downstream end to the plateau point, or from this plateau point to the upstream composition.

In principle, the slope of the isotherm of any binary couple of cations that participates in the chromatographic sequence can be inspected to see whether a shock or a broadening front will occur. If dq/dc increases in the upstream direction, a wave develops. If it decreases, a shock occurs. Rule based sequences can be given (Vermeulen et al., 1984). For example, the selectivity of natural exchangers for Na^+, K^+, Mg^{2+} and Ca^{2+} increases in the given order (Table 1). When, going upstream from x_{H_2O}, a decrease of an ion is accompanied by increase of a less selected ion, a wave develops. When it is accompanied

by increase in concentration of a more selected ion, a shock occurs. In terms of eigenvalues (or flushing factors + 1) of the system the following holds for the k^{th} transition (Charbeneau, 1988; cf. Figure 15, c^p is the plateau composition at the intersection point).

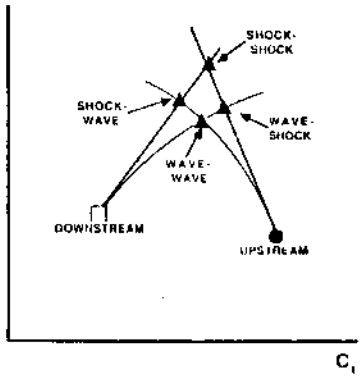

Figure 15. Possible locations of intersection points (plateaux) of two eigenvectors [Used by permission of the editor of *Water Resources Research*, from Charbeneau (1988)].

wave-wave:
$$\lambda_{k+1}(c^u) \geq \lambda_{k+1}(c^p) > \lambda_k(c^p) \geq \lambda_k(c^d)$$
wave-shock:
$$\lambda_{k+1}(c^u) \geq \lambda_{k+1}(c^p) > \lambda_k(c^p) < \lambda_k(c^d)$$
shock-wave:
$$\lambda_{k+1}(c^u) < \lambda_{k+1}(c^p) > \lambda_k(c^p) \geq \lambda_k(c^d)$$
shock-shock:
$$\lambda_{k+1}(c^u) < \lambda_{k+1}(c^p) > \lambda_k(c^p) < \lambda_k(c^d) \tag{34}$$

[The sequences will be illustrated below.]

For a system with all cations of the same charge (homovalent exchange) all the paths can be made straight by suitable mapping (Helfferich and Klein, 1970; Rhee et al., 1970, 1989). It is obtained setting the parameters θ and κ_i:

$$\theta = 1 + \sum_{i=1}^{n} c_i K_{iv} \tag{35}$$

and

$$\kappa_i = c_i(K_{iv} - 1) \tag{36}$$

so that

$$\beta_j = \frac{c_j}{\sum_{i=1}^{n} c_i K_{ij}} = \frac{\kappa_j K_{jv}}{\theta(K_{jv} - 1)} \tag{37}$$

This makes β_j a simple function of θ. The further development requires rather elaborate calculations, cf. Rhee et al. (1989).

For a heterovalent system, which will be most often encountered in nature, the paths are curved, and Equation (33) needs to be integrated. This can be done as shown by

Charbeneau for a system with three cations, and therefore with two eigenvectors. The integral is:

$$c^{k+1} = c^k + \int_{\theta_k}^{\theta_{k+1}} r^k \, d\theta \tag{38}$$

It can be approximated, using the trapezoidal rule:

$$c^{k+1} = c^k + \frac{1}{2}[r^k(c^k) + r^k(c^{k+1})]\Delta\theta_k \tag{39}$$

where $\Delta\theta_k = \theta_{k+1} - \theta_k$. With the notation $r^i(k)$ representing the average i^{th} eigenvector along the k^{th} composition path, (38) can be written

$$c^{k+1} = c^k + \Delta\theta_k r^i(k) \tag{40}$$

Thus, $r^i(k)$ is the i^{th} eigenvector, averaged in the k^{th} characteristic direction. There is one Equation (40) for each composition path. They are connected by the requirement that

$$c^{inj} - c^{init} = \sum_{j=1}^{n-1} \Delta\theta_j r^j(j) \tag{41}$$

Charbeneau (1988) has solved Equation (40) and (41) for two 3-cation systems, the laboratory experiment of Rainwater et al. (1987) and the field injection of Valocchi et al. (1981a, b). The latter will be discussed fully in the following parts. In principle, the sharp front Equations (26) and the differential Equation (33) for a broadening wave can be used for systems with more than 3 cations. This approach is now being implemented in a computer program (Van Veldhuizen and Hendriks, pers. comm.). The great advantage is that an exact solution is obtained of the chemical process during transport, without ghost peaks that may arise due to numerical oscillations, or spreading due to artificial dispersion that sometimes hamper the more common numerical solutions. Also, this program indicates exactly whether a shock or a wave occurs.

FIELD EXAMPLES OF ION CHROMATOGRAPHY

The case of Valocchi et al. (1981)

Valocchi et al. (1981a,b) injected fresh water in a brackish water aquifer shown in outline in Figure 16. The *CEC* of the recharged silty sand aquifer was 750 meq/l. The native brackish water had high Na^+ and Mg^{2+} concentrations, while the recharge water composition was dominated by Na^+ and Ca^{2+} but at about 10 times lower concentrations. Table 5 gives the water compositions, the exchangeable cations associated with these water compositions, and the difference in the exchangeable cation concentrations.

The injection of fresh water is accompanied by a loss of Na^+ and Mg^{2+} from the exchanger, and an increase of $Ca\text{-}X_2$. It is of interest to note that this loss of Na-X takes place although Na^+ as percentage of the three cations is higher in the injected water than in the native water. This is entirely due to the lower salinity of the injected solution. In equilibrium with a given exchanger composition, the solute ratios $[Na^+]/[Mg^{2+}]$ and $[Na^+]/[Ca^{2+}]$ remain the same, independent of the salinity of the solution as follows from Equation (5). When Na^+ is diluted 6.5 times from 86.5 to 13.3 mmol/l, Mg^{2+} and Ca^{2+} are diluted $(6.5)^2 = 42$ times, cf. Table 5.

Table 5. Mass balance calculations for exchanging ions in the injection experiment by Valocchi et al. (1981a): observation well S23. Concentrations in mmol/l.

Ion	Water			Sediment		
	Initial	Diluted	Injected	Initial	Injected	DIF
Na^+	86.5	13.3	9.4	160	56	+104
Mg^{2+}	18.2	0.43	0.5	142	41	+101
Ca^{2+}	11.1	0.26	2.13	153	306	-153

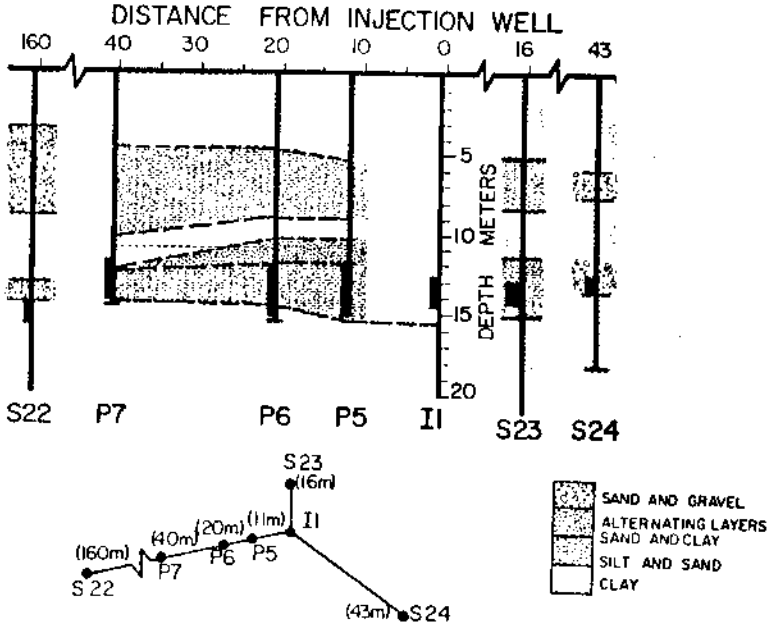

Figure 16. Outline of aquifer used for injecting fresh water by Valocchi et al. (1981a). [Used by permission of the editor of *Water Resources Research*.]

In this three-cation case, two eigenvectors must be followed from the initial to the injected composition, and one intermediate composition should be found between the (diluted) initial and injected compositions. Because it involves a displacement of Na^+ and Mg^{2+} by Ca^{2+}, and because Ca^{2+} is selected above the other two cations, the slope of the isotherm of any of the two binary pairs decreases in the upstream direction. Therefore, shock fronts are expected.

Figure 17 shows the trace of the Mg^{2+} and Ca^{2+} concentrations observed by Valocchi et al. (1981a) in well S23 at 16 m from the injection well. The full line is the computer simulation by Valocchi et al., the dotted is line a chromatographic pattern calculated for sharp fronts by Appelo et al. (1993). Concentrations drop when one pore volume (295 m^3 from injection well to S23) has been injected (the value of 295 m^3 was found by numerical

modeling of the Cl^- breakthrough curve; Appelo et al. used 260 m^3). The Ca^{2+} and Mg^{2+} concentrations remain at the (diluted) initial equilibrium concentrations until the first shock arrives with $V^* = 25.3$ (after $25.3 \times 295 + 295 = 7758$ m^3). Then the Na^+ concentration drops to almost the final concentrations, and the surplus of Mg^{2+} is flushed from the exchanger until the final concentration arrives with $V^* = 113.2$ (after $113.2 \times 295 + 295 = 33689$ m^3).

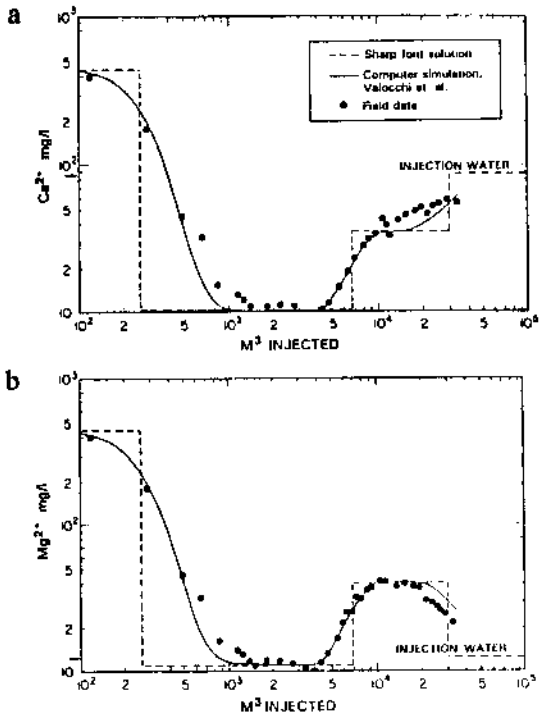

Figure 17. Concentrations of Ca^{2+} and Mg^{2+} in water from observation well S23 during injection of fresh water (Valocchi et al., 1981). The results of the sharp front approximation are shown hatched [Used by permission of the editor of the *Journal of Hydrology*, from Appelo et al. (1993)].

The condition for a shock front is given by Equation (34). Eigenvalues (flushing factors) are smaller for the upstream composition (which arrives later at the observation point). Figure 18 shows the eigenvalues for the three compositions of the Valocchi case and the transitions at the shock fronts. The first shock is pushed by $(V^*_1)_2 < (V^*_1)_1$. The second shock similar by V^*_2. Since also $V^s_2 > V^s_1$, the criteria for shock fronts are fully met.

Side reactions in the Valocchi case. Valocchi et al. did not refer to minerals in the aquifer, but calcite is ubiquitous and can be expected to be present. The decrease of Ca^{2+} concentrations during the chromatographic sequence will then be compensated by calcite dissolution:

$$H^+ + CaCO_3 \rightarrow Ca^{2+} + 2\,HCO_3^- \qquad (42)$$

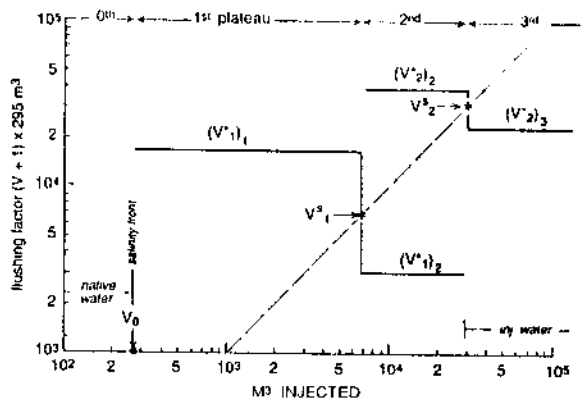

Figure 18. Flushing factors V^* and V^s for compositions of the Valocchi case. Hatched line indicates where flushing factor $(V + 1)$ is equal to injected volume. Note that $V^* + 1 = \lambda$. [Used by permission of the editor of the *Journal of Hydrology*, from Appelo et al. (1993)].

The increased availability of Ca^{2+} will accelerate the chromatographic sequence. This also follows from the smaller change $V^* = \Delta q_{Ca}/\Delta c_{Ca}$, since

$$\Delta q_{Ca} = \Delta Ca\text{-}X_2 + \Delta CaCO_3 \qquad (43)$$

where $\Delta CaCO_3$ is the change in calcite concentration in the aquifer sediment (expressed as mol/l pore water). It is possible to calculate fronts for a combination of exchange and dissolution and precipitation (Harmsen and Bolt, 1982; Bryant et al., 1987; cf. also Lefèvre et al., 1993). Here, we illustrate the effect with a numerical simulation of the complete reaction, assuming that calcite is not exhausted

In principle the loss of Ca^{2+} from solution is sufficient to drive the dissolution reaction. However, the amount that dissolves is small, because pH rapidly increases to 10. This is not observed in aquifers, because of proton buffering. Reaction (42) indicates that some form of proton buffering will be present, that will keep pH at about 7 to 8. Proton buffering may be due to desorption of protons from oxides and organic matter, or perhaps due to desorption of complexes, in combination with reaction of oxides (Griffioen, 1993). For the model calculation done here, it was assumed that a constant CO_2 pressure of 0.01 atm was the source of protons. Figure 19 shows model results obtained with the hydrogeochemical transport model PHREEQM (Appelo and Postma, 1993) when the exchange reaction and the calcite equilibrium reaction are both included.

About 0.94 mmol/l calcite dissolves over the interval of the chromatographic sequence which lasts 170 pore volumes. This amounts to $170 \times 0.94 \times 295 = 47.14$ kmol calcite in total. Figure 19 also shows the modeled Ca^{2+} concentration for the case without calcite dissolution. The main difference lies in the higher Ca^{2+} concentration in the initial dilution plateau that is reached when calcite equilibrium is included, and also in that the complete reaction finishes more rapidly. However, the overall pattern is not much different, which points to the dominance of the cation exchange reaction. One may speculate that dissolution of calcite has been an actual reaction in the Valocchi experiment. In that case the exchange capacity will be probably somewhat higher (CEC = 1000 meq/l) than noted by Valocchi et al. (1981a).

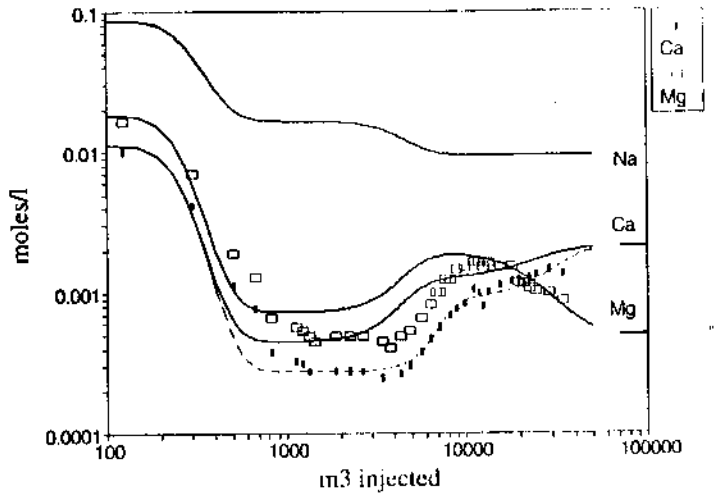

Figure 19. Modeling the Valocchi et al. injection with the hydrogeochemical transport model PHREEQM, ion exchange and calcite dissolution, P_{CO_2} = 0.01 atm. Thin dotted line is Ca^{2+} concentration in a model without calcite equilibrium.

Inverting water compositions. It is interesting to invert the water compositions in the Valocchi case and inject brackish water into a fresh aquifer. The initial composition is given in Table 6. Now Na^+ and Mg^{2+} increase in the upstream direction, and Na-X and Mg-X_2 must increase at the cost of Ca-X_2. Figure 20 shows the solute concentrations for the ideal chromatographic case without dispersion.

Table 6. Inverted compositions for the injection experiment by Valocchi et al. (1981a): Brackish water into fresh water aquifer. Concentrations in mmol/l.

Ion	Water Initial	Diluted	Injected
Na^+	9.4	41.6	86.5
Mg^{2+}	0.5	9.83	18.2
Ca^{2+}	2.13	41.9	11.1

There are two eigenvectors and one plateau composition. Because the less selected ions increase upstream, the paths are waves. The first one starts when the first eigenvalue of the first composition is equal to the number of pore volumes that have been injected $[(V^*_1)_1 + 1 = 2.56]$. It goes on until the first plateau composition is reached $[(V^*_1)_2 + 1 = 3.46]$. This composition is maintained until the second eigenvalue is equal to the injected pore volumes. Then the second eigenvector is followed up to the injected composition. The development of the eigenvalues for this system is given in Figure 21. Note that the overall response is much quicker than in the real case discussed earlier, because higher concentrations in the injected solution allow a larger Δc.

Effects of salinity pulses

The response to groundwater salinity changes is clearest with a dilution because Δc's are limited by N, and the flushing factors are accordingly larger. It can nevertheless be observed in the passage of the salt pulse when the exchangeable cations continue to dominate over solute cations (Bjerg et al., 1993; Ceazan et al., 1989). Ceazan et al. (1989) injected NH_4Br in an aquifer and analyzed the passage of the pulse in an observation well 1.5 m downstream. The arrival of Br^- was accompanied by an increase of N from 0.5 to

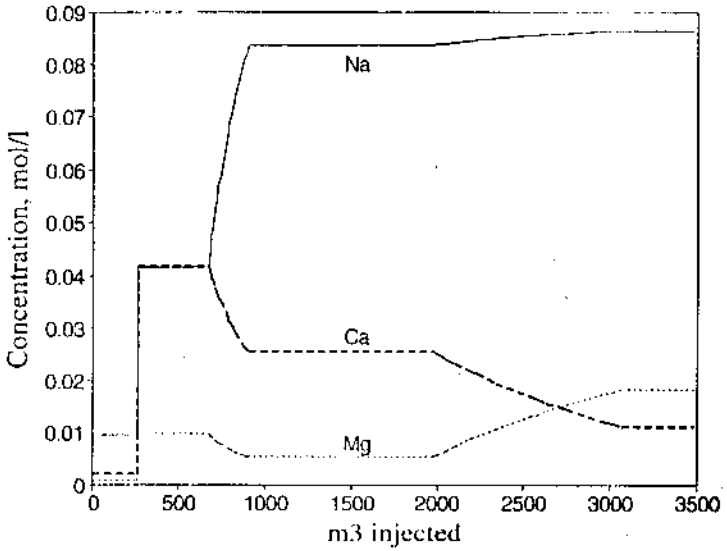

Figure 20. Concentrations in the Valocchi case when brackish water is injected in the fresh aquifer. Based on calculations with MIE (Van Veldhuizen and Hendriks, pers. comm.).

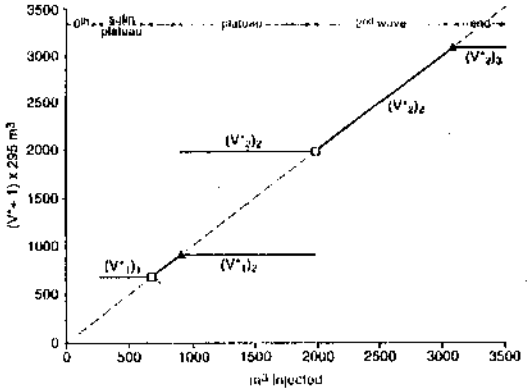

Figure 21. Flushing factors $(V^* + 1)$ for the inverted Valocchi case. Eigenvector path starts at □ and ends at ▲.

1.8 meq/l, as shown in Figure 22. The ratio of the divalent cations over Na^+ changed from 0.33 in the native water to a maximum of 0.78 at the peak of the Br^- concentration, strictly conforming to Equations (5) and (7) (Fig. 23).

Salinity pulses are naturally occurring in soils during sequences of dry and wet years. A particular example has been noted by Hansen and Postma (1995) in a 4 to 5 m thick unsaturated zone near the coast of Denmark. Acidification has caused dissolution of Al^{3+} from minerals in the sand, and Al^{3+} concentrations as high as 0.8 mmol/l were observed. When in a dry year the Cl^- concentration increases, equilibrium with the exchange complex requires that Al^{3+} increases by n^3 when Na^+ increases by n. Because the Al^{3+} concentration in the soil solution is in equilibrium with gibbsite, the increase leads to precipitation of

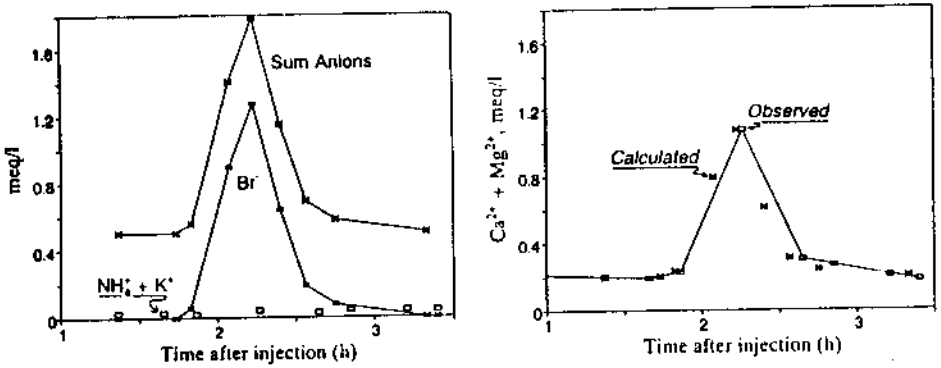

Figure 22 (left). Concentrations of ions in the NH_4Br injection experiment of Ceazan et al. (1989).

Figure 23 (right). The observed (□) and calculated (×) concentrations of Ca^{2+} and Mg^{2+} during the passage of the Br^- peak in the injection experiment of Ceazan et al. (1989). [Figures 22 and 23 used by permission of the editor of *Ground Water*, from Appelo (1994b)].

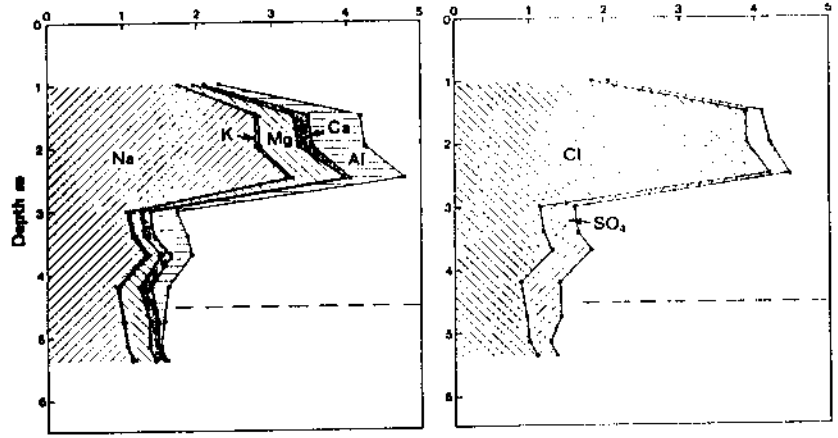

Figure 24. Solute concentrations with depth in an acidified profile at Klosterhede. The hatched line gives the groundwater table. [Used by permission of the editor of *Water Resources Research*, from Hansen and Postma (1995)].

$Al(OH)_3$. Consequently, OH^- is removed from solution, and the salt pulse is at the same time an acid pulse.

Figure 24 shows an observed profile, note that Al in the soil solution is highest at the highest Cl^- concentration. Figure 25 shows calculations of a salt pulse through the profile, with cation exchange and gibbsite equilibrium. Essentially the reaction mechanism is as noted above. The solute concentrations of the salt pulse rapidly equilibrate with the exchange complex in the upper part of the profile. Na^+ is sorbed, and Mg^{2+} and particularly Al^{3+} are desorbed. The equilibrated composition then travels indifferently through the soil. Figure 25 shows the composition when the salt pulse has arrived at -4 m. Note that the exchangeable cations do not change over the salt pulse but that the relative proportions of the solute ions differ quite markedly.

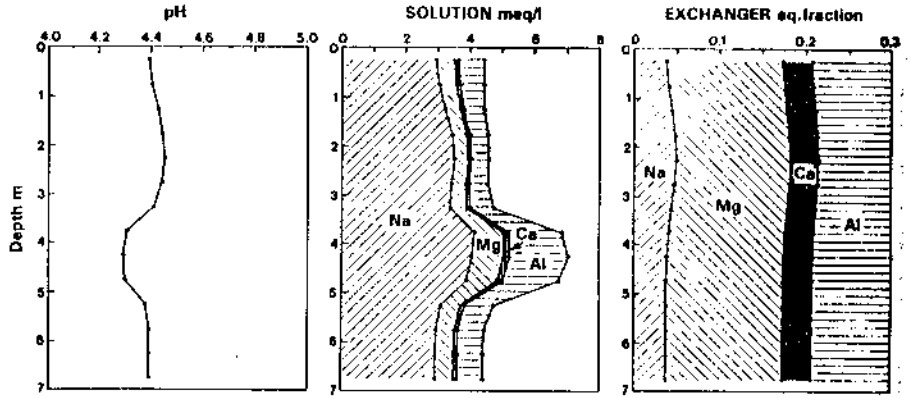

Figure 25. Modeling the movement of a salt pulse through an acidified profile. The pulse had doubled NaCl at zero depth. [Used by permission of the editor of *Water Resources Research*, from Hansen and Postma (1995)].

Freshening of saline aquifers

$NaHCO_3$ waters are found in many Tertiary aquifers along the coast of western Europe (Walraevens and Cardenal, 1994) and eastern U.S.A. (Foster, 1950; Back, 1966; Chapelle and Knobel, 1983). The water quality has been related to cation exchange of Na^+ for Ca^{2+} from fresh $Ca(HCO_3)_2$ water. The freshening of the (initially) saline aquifers was induced by the drop of sea level during the Pleistocene. The aquifers also contain $Mg(HCO_3)_2$ waters, which have been related to transformation of Mg-calcite into a purer carbonate (Chapelle and Knobel, 1983). An attractive alternative to the carbonate reactions is to assume a chromatographic sequence similar to the Valocchi case (Appelo, 1994a). A soil exchanger in equilibrium with seawater has also increased Mg-X_2 (cf. Fig. 2 and Fig. 3). Freshening will lead to a sequence in which Na^+ is removed first and then Mg^{2+}.

The sequence is present in an exemplary form in the Aquia aquifer (Maryland, U.S.A.). The aquifer is shown in outline in Figure 26. Observed water qualities along an averaged flowpath even show a K^+ peak between the high Na^+ and Mg^{2+} concentrations (Fig. 27). The pattern could be modeled as a cation exchange process, as shown by the model lines in Figure 27.

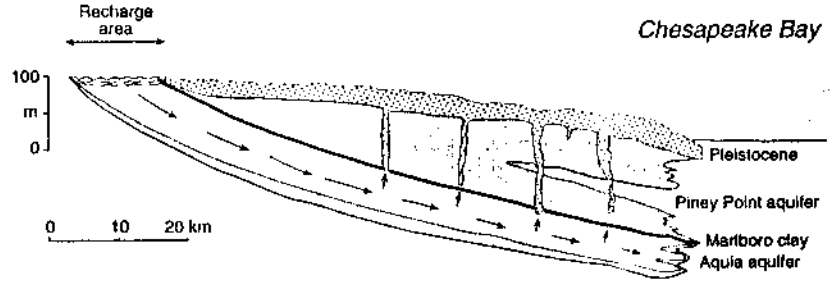

Figure 26. Cross section of the Aquia aquifer, Maryland, USA. [Used by permission of the editor of *Water Resources Research*, from Appelo (1994b)].

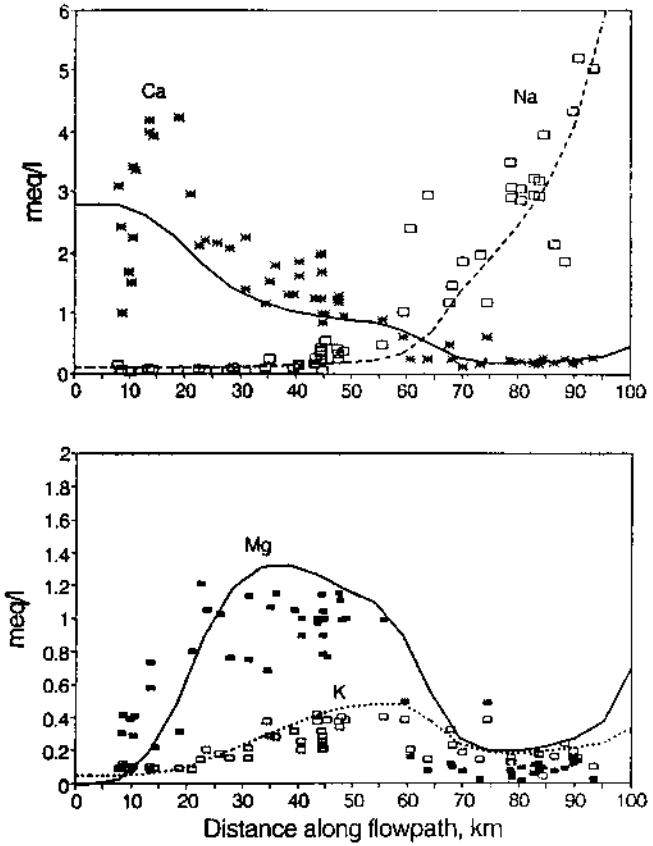

Figure 27. Along an average flowpath in the Aquia aquifer, a sequence of Na^+, K^+, Mg^{2+} and Ca^{2+} concentration peaks are observed that can be modeled as a chromatographic sequence. Data points from Chapelle and Knobel (1983).

The Aquia aquifer is probably the most ideal natural analogue of a laboratory column. Its thickness is less than 100 m over a length of 90 km (Fig. 26), which makes it similar to a hair-thin chromatographic column of, say 1 dm length. Dispersion is therefore relatively reduced and the chromatographic transitions remain visible. The sharpness of the pattern is also preserved because during freshening all the transitions are shocks. Dispersion that is inevitable at the scale of an aquifer, is counteracted by the cation exchange reaction. The pattern is apparently stable over the 100 ka that were calculated to be necessary for its establishment (Appelo, 1994a).

Diffusion profiles tend to show only reduced chromatographic separations in space, because diffusion of the exchange forcing cations is about as rapid as the exchanged cations (Appelo and Willemsen, 1987). However, the salinity effect is very clear in a fresh water diffusion profile observed by Manzano et al. (1992). Manzano et al. (1992) extracted pore water from a silty Holocene aquitard in the Llobregat delta in Spain. The aquitard contains saline water and is freshening from below by diffusion of fresh water from the underlying

aquifer. The measured cation concentrations are compared with concentrations calculated for conservative mixture of fresh and saline water in Figure 28.

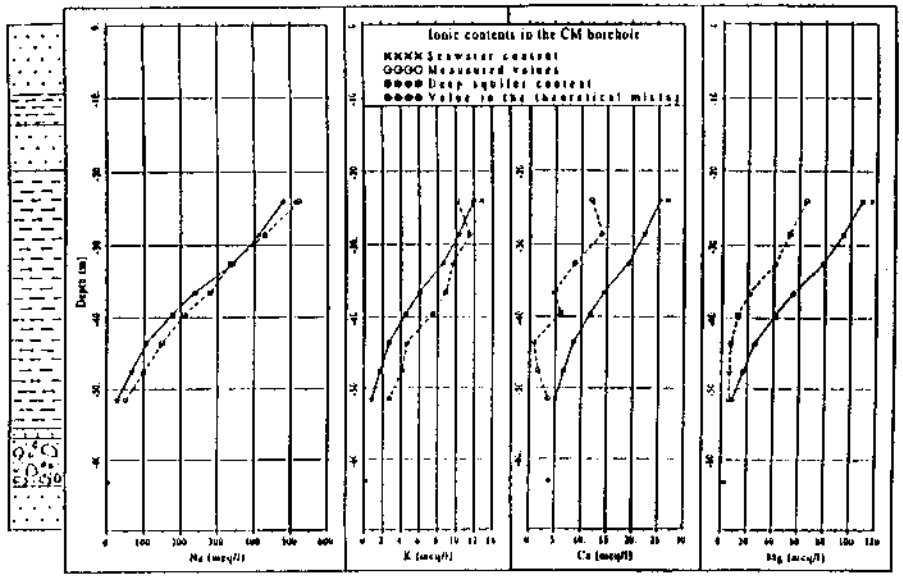

Figure 28. Analyzed (o——o) and theoretical mixed (•——•) water compositions in the upper aquitard of the Llobregat delta. [From Manzano et al. (1992)].

The initial effect of diffusion in this case is a dilution of pore water. The dilution is accompanied by relative increase of the monovalent ions and a decrease of the divalent ions. The changes are relative to a conservative mixing and are identical to the examples discussed earlier. The Ca^{2+} concentration decreases here to below the fresh water concentration, similar to the Valocchi case. Manzano et al. have modeled the concentration profiles and observed that varying K_{Ni} for the exchange reaction had only minor influence on the calculated solute profiles. This can now be understood fully, because in the model calculations the solute ratio $i^+/\sqrt{j^{2+}}$ is constant by the exchange equilibrium with $K_{Ni}\beta_i/\sqrt{\beta_j}$ (Eqn. 5). The latter quotient is balanced by the (constant) initial saline water composition, in which the ratios of the β's compensate for changes in K_{Ni}. This will change the available mass of i-X_z, but these are only noted with transport and in the onset of the next composition path that is followed in the chromatographic pattern.

SUMMARY

We presented an overview of chromatographic effects on natural water qualities. We started with multicomponent ion exchange and have shown that simple equilibrium calculations are valid for natural waters and (correctly) measured exchangeable cations. Chromatography involves the separation of ions due to different transport velocities for different concentrations. The fundamental equation for calculating transport velocity is mass balance. Most simply, it can be stated in the form $dq = V\,dc$. It contends that a change in sorbed concentration must go with a change in solution concentration over a fixed

solution volume (or time). The change in solution concentration can be infinitesimal as in the equation, and it will lead to a wave; the solution volume is given by the change of slope of the isotherm dq/dc. It can also be finite, and the solution volume is given by $\Delta q/\Delta c$; this will give a shock-like change in concentrations. For multicomponent exchange and transport, the dq/dc term must be equal for all solutes that participate in the solid-solution equilibria. This relationship can be exploited to deduce chromatographic waves and shocks, the separations of ions, and the velocity of compositions and composition transitions in general. Advances in the mathematical description of these systems have been presented. They were found to be applicable to various hydrochemical field situations with transient water qualities.

In many natural settings the effects of a salinity pulse are the most obvious. These can be simply calculated. The ratio of heterovalent ions in solution after a change in total concentration (eq/l) are found from:

$$\left(\frac{c_i^{1/z_i}}{c_j^{1/z_j}}\right) = \text{constant} \qquad (44)$$

When the salinity pulse develops into a block, a full chromatographic sequence will be observed. These sequences were illustrated for the three cation injection cases of Valocchi et al. (1981a,b) and for a freshening aquifer.

Symbols

Greek letters

β_i	Equivalent fraction of *CEC* occupied by cation *i* (-)
ε	(Water filled) porosity (-)
θ	Self-similar variable, $\theta = \theta(c, (vt/x))$ (mol/l)
λ	Eigenvalue of the matrix $(I + Q)$ (-)
ρ_b	Bulk density (g/cm^3)

Latin letters

c_i	Solute concentration of *i* (mol/l)
c	Vector of solute concentrations
CEC	Cation exchange capacity (meq/100g soil, or mol$_c$/l pore water)
I	Identity matrix
N	Total cations of the solution (eq/l)
Q	Coefficient matrix of multicomponent exchange $(\partial q_i/\partial c_j)_{i,j=1,\ldots,n-1}$
q_i	Sorbed or exchangeable concentration of *i* (mol/l pore water)
r^k	k^{th} eigenvector
V^*	Flushing factor (-)
V^*	Sharp front flushing factor (-)
v	Pore water flow velocity (m/s)
z_i	Charge on ion i^{z_i+}

ACKNOWLEDGMENTS

Peter Lichtner and Rien van Veldhuizen are gratefully acknowledged for critical reading of the manuscript. The EEC funded Palaeaux project provided financial support.

REFERENCES

Appelo CAJ, Willemsen A (1987) Geochemical calculations and observations on salt water intrusions. I. J Hydrol 94:313-330
Appelo CAJ, Willemsen A, Beekman HE, Griffioen J. (1990) Geochemical calculations and observations on salt water intrusions. II. J Hydrol 120:225-250
Appelo CAJ, Hendriks JA, Van Veldhuizen M (1993) Flushing factors and a sharp front solution for solute transport with multicomponent ion exchange. J Hydrol 146:89-113
Appelo CAJ, Postma D (1993) Geochemistry, Groundwater and Pollution. Balkema, Rotterdam, 536 p
Appelo CAJ (1994a) Cation and proton exchange, pH variations, and carbonate reactions in a freshening aquifer. Water Resources Res 30:2793-2805
Appelo CAJ (1994b) Some calculations on multicomponent transport with cation exchange in aquifers. Ground Water 32:968-975
Appelo CAJ, Verweij E, Schäfer H (1996) A hydrogeochemical transport model for an oxidation experiment with pyrite/calcite/exchangers containing sand. Geochim Cosmochim Acta (submitted)
Back W (1966) Hydrochemical facies and groundwater flow patterns in northern part of Atlantic coastal plain. US Geol Surv Prof Paper 498-A, 42 p
Beekman HE (1991) Ion chromatography of fresh- and seawater intrusion. PhD dissertation, Free Univ, Amsterdam, 198 p
Beekman HE, Appelo CAJ (1990) Ion chromatography of fresh- and salt-water displacement: laboratory experiments and multicomponent transport modeling. J Contam Hydrol 7:21-37
Bichkova VA, Soldatov VS (1985) A method for predicting ion exchange equilibria in ternary ion exchange systems. React Polymers 3:207-215
Bjerg PL, Ammentorp HC, Christensen TH (1993) Model simulations of a field experiment on cation exchange-affected multicomponent solute transport in a sandy aquifer. J Contam Hydrol 12:291-311
Bolt GH (1967) Cation exchange equations used in soil science - a review. Neth J Agric Sci 15:81-103
Bolt GH (ed) (1982) Soil Chemistry. B. Physico-Chemical Models. Elsevier, Amsterdam, 527 p
Bond WJ, Phillips IR (1990) Approximate solutions for cation transport during unsteady, unsaturated soil water flow. Water Resources Res 26:2195-2205
Bruggenwert MGM, Kamphorst A (1982) A survey of experimental information on cation exchange in soil systems. In Bolt GH (ed) Soil Chemistry, B. Physico-Chemical Models. 141-203. Elsevier, Amsterdam
Bryant SL, Schechter RS, Lake LW (1986) Interactions of precipitation/dissolution waves and ion exchange in flow through permeable media. Am Inst Chem Eng J 32:751-764
Bürgisser C, Cernik M, Borkovec M, Sticher H (1993) Determination of nonlinear adsorption isotherms from column experiments: an alternative to batch studies. Environ Sci Technol 27:943-948
Bürgisser C, Scheidegger AM, Borkovec M, Sticher H (1994) Chromatographic charge density determination of materials with low surface area. Langmuir 10:855-860
Ceazan ML, Thurman EM, Smith RL (1989) Retardation of ammonium and potassium transport through a contaminated sand and gravel aquifer: the role of cation exchange. Environ Sci Technol 23:1402-1408
Cernik M, Barmettler K, Grolimund D, Rohr W, Borkovec M, Sticher H (1994) Cation transport in natural porous media on laboratory scale: multicomponent effects. J Contam Hydrol 16:319-337
Chapelle FH, Knobel LL (1983) Aqueous geochemistry and exchangeable cation composition of glauconite in the Aquia aquifer, Maryland. Ground Water 21:343-352
Charbeneau RJ (1981) Groundwater contaminant transport with adsorption and ion exchange chemistry: method of characteristics for the case without dispersion. Water Resources Res 17:705-713.
Charbeneau RJ (1988) Multicomponent exchange and subsurface solute transport: characteristics, coherence, and the Riemann problem. Water Resources Res 24:57-64.
DeVault D (1943) The theory of chromatography. J Am Chem Soc 65:532-540.
DeZabala EF, Vislocky JM, Rubin E, Radke CJ (1982) A chemical theory for linear alkaline flooding. Soc Petrol Eng J 245-258
Duncan JF, Lister BAJ (1949) Ion exchange studies. I. The sodium-hydrogen system. J Chem Soc (London) 3285-3296
Ekedahl E, Högfeldt E, Sillén LG (1950) Kinetics and equilibria of ion exchange. Nature 166:723-724
Elprince AM, Babcock KL (1975) Prediction of ion-exchange equilibria in aqueous systems with more than two counter-ions. Soil Sci 120:332-338.
Faucher JA, Southworth RW, Thomas HC (1952) Adsorption studies on clay minerals. I Chromatography on clays. J Chem Phys 20:157-160
Faucher JA, Thomas HC (1954) Adsorption studies on clay minerals. IV The system montmorillonite-cesium-potassium. J Chem Phys 22:258-261

Foster MD (1950) The origin of high sodium bicarbonate waters in the Atlantic and Gulf coastal plains. Geochim Cosmochim Acta 1:33-48
Franklin KR, Townsend RP (1988) Multicomponent ion exchange in zeolites. Pt 3 Equilibrium properties of the sodium/potassium/cadmium—zeolite X system. J Chem Soc Faraday Trans I 84:687-702
Gaines GL, Thomas HC (1953) Adsorption studies on clay minerals. II. A formulation of the thermodynamics of exchange adsorption. J Chem Phys 21:714-718
Glückauf J (1945) Adsorption isotherms from chromatographic measurements. Nature 156:748
Glückauf J (1949) Theory of chromatography. VI Precision measurements of adsorption and exchange isotherms from column-elution data. J Chem Soc (London) 3280-3285
Glückauf J (1955) Principles of operation of ion-exchange columns, in: Ion exchange and its applications. Soc Chem Ind (London) 34-46
Griffioen J (1993) Multicomponent cation exchange including alkalinization/acidification following flow through sandy sediment. Water Resources Res 29:3005-3019
Griffioen J, Appelo CAJ, Van Veldhuizen M (1992) Practice of chromatography: deriving isotherms from elution curves. Soil Sci Soc Am J 56:1429-1437
Groen KP (1991) History of Salt Water Investigations in The Netherlands (in Dutch). Flevobericht 321, Min van Waterstaat, Lelystad
Hansen BK, Postma D (1995) Acidification, buffering, and salt effects in the unsaturated zone of a sandy aquifer, Klosterhede, Denmark. Water Resources Res 31:2795-2809
Harmsen K, Bolt GH (1982) Movement of ions in soil. I. Ion exchange and precipitation. Geoderma 28:85-101
Harmsen K, Bolt GH (1982) Movement of ions in soil. II. Ion exchange and dissolution. Geoderma 28:103-116
Helfferich F (1967) Multicomponent ion exchange in fixed beds. Ind Eng Chem Fund 6:362-364
Helfferich F, Klein G (1970) Multicomponent Chromatography. M Dekker, New York,
Hofstee J (1971) Methods of Analysis (in Dutch). Rijksdienst IJsselmeerpolders, Kampen, The Netherlands
Klein G, Tondeur D, Vermeulen T (1967) Multicomponent ion exchange in fixed beds. Ind Eng Chem 6:339-351
Kool JB, Parker JC, Zelazny LW (1989) On the estimation of cation exchange parameters from column displacement experiments. Soil Sci Soc Am J 53:1347-1355
Lax P (1957) Hyperbolic systems of conservation laws II. Comm Pure Appl Math 10:537-566
Lax P (1973) Hyperbolic Systems of Conservation Laws and the Mathematical Theory of Shock Waves. S I A M, Philadelphia, PA, 48 p
Lindstrom FT, Haque R, Freed VH, Boersma L (1967) Theory on the movement of some herbicides in soils: linear diffusion and convection of chemicals in soils. J Environm Sci Tech 1:561-565
Lefèvre F, Sardin M, Schweich D (1993) Migration of strontium in clayey and calcareous sandy soil: precipitation and ion exchange. J Contam Hydrol 13:215-229
Mansell RS, Bloom SA, Bond WJ (1993) A tool for evaluating a need for variable selectivities in cation transport in soil. Water Resources Res 29:1855-1858
Mangold DC, Tsang C-F (1991) A summary of subsurface hydrological and hydrochemical models. Rev Geophys 29:51-79
Manzano M, Custodio E, Carrera J (1992) Fresh and salt water in the Llobregat delta aquitard. Proc 12th Saltwater Intrusion Mtg, Barcelona. CIMNE, Barcelona, 207-238
Merriam CN, Southworth RW, Thomas HC (1952) Ion exchange mechanism and isotherms from deep bed performance. J Chem Phys 20:1842-1846
Merriam CN, Thomas HC (1956) Adsorption studies on clay minerals. VI. Alkali ions on attapulgite. J Chem Phys 24:993-995
Page AL, Miller RH, Keeney DR (1982) Methods of soil analysis. Pt 2. Chemical and Microbiological Properties, 2nd edition. Soil Sci Soc Am, Madison, Wisconsin, 1159 p
Parkhurst DL (1995) User's guide to PHREEQC - A computer program for speciation, reaction-path, advective transport, and inverse geochemical calculations. U S Geol Surv Water Resources Inv 95-4227, 143 p
Pope GA, Lake LW, Helfferich FG (1978) Cation exchange in chemical flooding: Part 1 - Basic theory without dispersion. Soc Petrol Eng J 418-433
Rainwater KA, Wise WR, Charbeneau RJ (1987) Parameter estimation through groundwater tracer tests. Water Resources Res 23:1901-1910
Rhee H-K, Aris R, Amundson NR (1970) On the theory of multicomponent chromatography. Phil Trans Roy Soc (London) 267A:419-455
Rhee H-K, Aris R, Amundson NR (1989) First order partial differential equations. Vol. II. Prentice Hall, Englewood Cliffs, NJ, 548 p

Ritchie AS (1966) Chromatography as a natural process in geology. In Giddings JC, Keller RA (eds) Adv Chromatogr 3:119-134. M Dekker, New York
Rubin J, James RV (1973) Dispersion-affected transport of reacting solutes in saturated porous media: Galerkin method applied to equilibrium-controlled exchange in unidirectional steady water flow. Water Resources Res 9:1332-1356
Scheidegger A, Bürgisser CS, Borkovec M, Sticher H, Meeussen H, Van Riemsdijk W (1994) Convective transport of acids and bases in porous media. Water Resources Res 30:2937-2944
Schweich D, Sardin M (1981) Adsorption, partition, ion exchange and chemical reaction in batch reactors or in columns—a review. J Hydrol 50:1-33
Schweich D, Sardin M, Gaudet J-P (1983) Measurement of a cation exchange isotherm from elution curves obtained in a soil column: preliminary results. Soil Sci Soc Am J 47:32-37
Schweich D, Sardin M, Jauzein M (1993) Properties of concentration waves in presence of nonlinear sorption, precipitation/dissolution, and homogeneous reactions. 1. Fundamentals. Water Resources Res 29:723-733
Sillén LG (1950) Theory of sorption columns. Nature 166:722-723
Sillén LG (1951) On filtration through a sorbent layer. IV. Arkiv Kemi 2:477-498
Smoller J (1983) Shock waves and reaction-diffusion equations. Springer-Verlag, New York
Sposito G (1994) Chemical equilibria and kinetics in soils. Oxford Univ Press, New York, 268 p
Stuyfzand PJ (1993) Hydrochemistry and hydrology of the coastal dune area of the Western Netherlands. PhD dissertation, Free Univ, Amsterdam, 366 p
Thoolen PMC, Heinker PW (1991) Approximation methods for n-component solute transport and ion-exchange. Rept 91-9, Dept Mathematics, Univ Amsterdam, 26 p
Tondeur D (1969) Théorie des colonnes d'échange d'ions. PhD dissertation, Nancy. 166 p
Valocchi AJ, Street RL, Roberts PV (1981a) Transport of ion-exchanging solutes in groundwater: chromatographic theory and field simulation. Water Resources Res 17:1517-1527
Valocchi AJ, Roberts PV, Parks GA, Street RL (1981b) Simulation of the transport of ion-exchanging solutes using laboratory-determined chemical parameter values. Ground Water 19:600-607
Van der Molen WH (1958) The Exchangeable Cations in Soils Flooded with Seawater. Staatsdrukkerij, Den Haag, 167 p
Van Veldhuizen M, Appelo CAJ, Griffioen J (1995) The (least-squares) quotient algorithm as a rapid tool for obtaining sorption isotherms from column elution curves. Water Resources Res 31:849-857
Van Veldhuizen M, Hendriks J (in prep) MIE, a computer program for analytical solution of multicomponent, heterovalent chromatography. Dept Mathematics, Free Univ, Amsterdam
Vermeulen Th, LeVan MD, Hiester NK, Klein G (1984) Adsorption and ion exchange. In: Perry's Chemical Engineer's Handbook, 6th edn, McGraw-Hill, New York, Ch 16.
Walraevens K, Cardenal J (1994) Aquifer recharge and exchangeable cations in a Tertiary clay layer (Bartonian clay, Flanders-Belgium). Mineral Mag 58A:955-956.
Yeh GT, Tripathi VS (1989) A critical evaluation of recent developents of hydrogeochemical transport models of reactive multichemical components. Water Resources Res 25:93-108
Zaur AJ (1938) In: Trans 2nd Comm and Alkali-Subcomm, Int'l Congress Soil Science, Helsinki B:66-67